The sedimentary and tectonic evolution of the Yinggehai–Song Hong basin and the southern Hainan margin, South China Sea: Implications for Tibetan uplift and monsoon intensification

Peter D. Clift[1,2] and Zhen Sun[3]

Received 13 September 2005; revised 29 December 2005; accepted 28 February 2006; published 22 June 2006.

[1] The Yinggehai–Song Hong basin is one of the world's largest pull-apart basins, lying along the trace of the Red River fault zone in the South China Sea. South of Hainan Island this basin crosscuts the rifted margin of the northern South China Sea. In this paper we present for the first time a regional compilation of multichannel seismic reflection data from both the strike slip and rifted margins. The basins started to open after ~45 Ma, especially after ~34 Ma. The Yinggehai basin was folded and inverted in the middle Miocene, after 21 Ma in the north and 14 Ma in the south, before rapidly subsiding again after ~5 Ma because of continued tectonism. This subsidence has caused shale diapirism, especially driven by associated sedimentation in the late Pliocene (2.6–2.0 Ma). Extension along the adjacent south Hainan margin shows preferential lower crustal extension, suggestive of lower crustal flow increasing toward the continent-ocean transition during breakup. Sediment supply is reconstructed to peak in the middle Miocene, then falls between 14 and 10.3 Ma to reach a low in the late Miocene. However, rates rose again in the Pliocene-Pleistocene. The Red River sediment budget is incompatible with climate models that propose stronger monsoon rains starting at 8 Ma or with large-scale river capture away from the Red River after ~10 Ma. Both lines of evidence point to major uplift in the Red River drainage being middle Miocene or older. The recent, preindustrial Red River carried much more sediment than the average Pleistocene accumulation rate, indicating modest sediment buffering onshore, at least in recent geologic time.

Citation: Clift, P. D., and Z. Sun (2006), The sedimentary and tectonic evolution of the Yinggehai–Song Hong basin and the southern Hainan margin, South China Sea: Implications for Tibetan uplift and monsoon intensification, *J. Geophys. Res.*, *111*, B06405, doi:10.1029/2005JB004048.

1. Introduction

[2] The uplift history of the Tibetan Plateau continues to be a contentious issue for Earth and ocean scientists, yet it is one of great importance to understanding how crust deforms in continental collision zones, as well as how the solid Earth and the climatic system interact. Crustal thickening under Tibet, triggered by the India-Eurasia collision, not only caused rock uplift at the point of collision but also appears to be linked to the development of a series of regional strike-slip faults, many of which run through Indochina and that push up mountain ranges and/or open basins [e.g., *Molnar and Tapponnier*, 1975; *Tapponnier et al.*, 1986; *Lacassin et al.*, 1997; *Leloup et al.*, 2001; *Morley*, 2002; *Replumaz and Tapponnier*, 2003]. In addition, plateau uplift has driven drainage reorganization and resulted in a number of the world's largest rivers running from eastern Tibet into the marginal seas of Asia [*Wang*, 2004]. These are fed by the monsoon rains that are often linked to the modern surface elevation of Tibet [*Prell and Kutzbach*, 1992; *Webster et al.*, 1998; *An et al.*, 2001]. The sedimentary sequences preserved in the marginal of basins of southeast Asia thus potentially hold the key to understanding how tectonic deformation, erosion and climate interact in this region.

[3] In this study we present newly released and analyzed seismic reflection profiles from the Yinggehai–Song Hong basin and its neighbor the Qiongdongnan basin, both located offshore southern Hainan Island in the South China Sea (Figure 1). The objective of our study is to reconstruct the tectonic evolution of these basins. The Yinggehai basin formed at the southern termination of the largest of the Tibetan strike slip zones, the Red River fault, while the Qiongdongnan basin formed as an extensional basin at the intersection between the Yinggehai strike-slip system and the main South China Sea basin. We also quantify and explain the nature of its sedimentary fill. The Yinggehai basin is the principal repository of material eroded in the Red River drainage and should be sensitive to changes in erosion rate in eastern Tibet, as well as to the loss of drainage from the modern Red River, which has been

[1] School of Geosciences, University of Aberdeen, Aberdeen, UK.
[2] Also at Deutsch Finnische Gesellschaft Research Center Ocean Margins (DFG-RCOM), Universität Bremen, Bremen, Germany.
[3] Key Laboratory of Marginal Sea Geology, South China Sea Institute of Oceanology, Chinese Academy of Sciences, Guangzhou, China.

0148-0227/06/2005JB004048$09.00

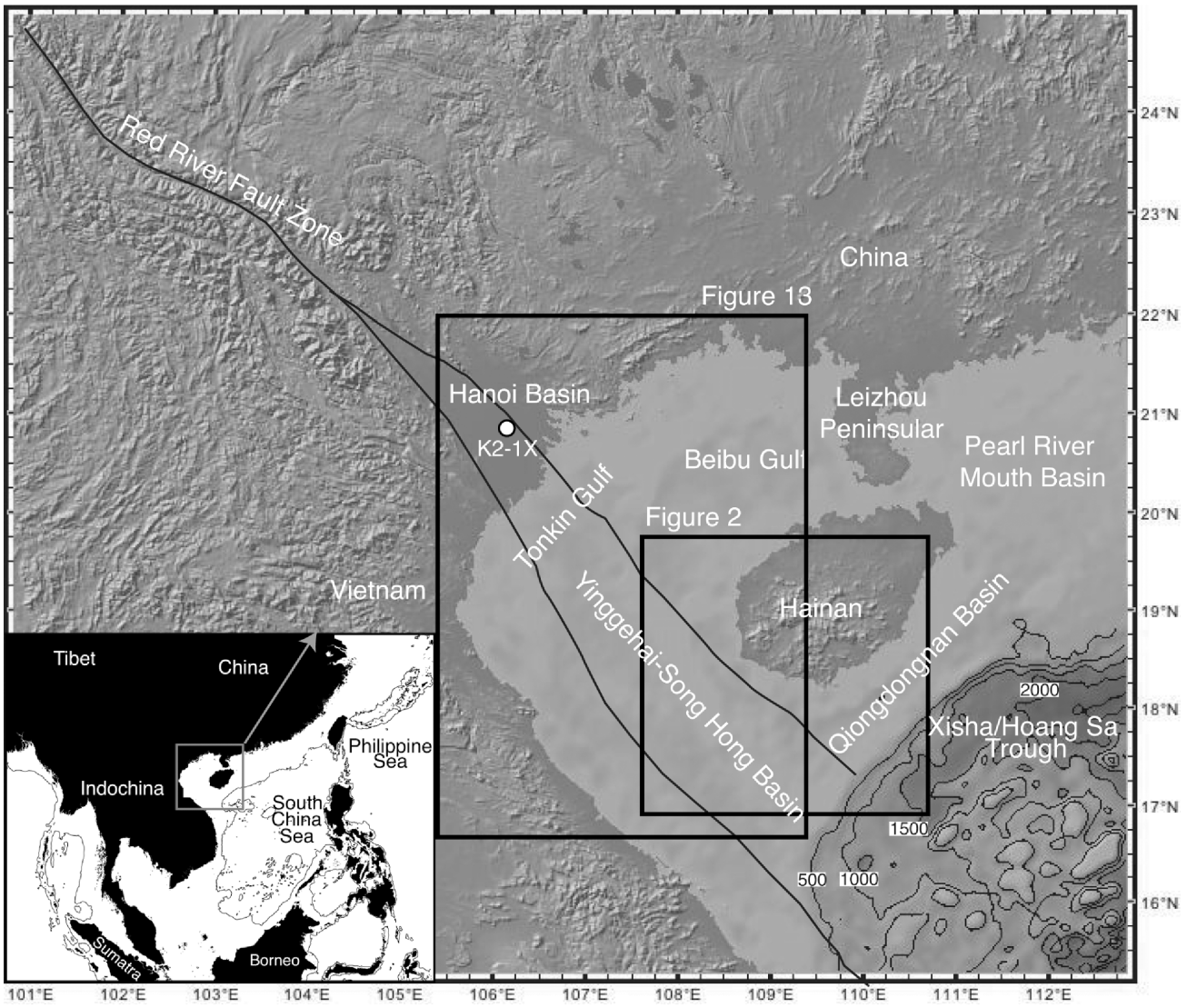

Figure 1. Shaded topographic and bathymetric maps of the region around the Yinggehai–Song Hong basin showing its relationship with the Red River fault zone onshore, with the structural high of Hainan Island, and with the deep water of the Xisha-Hoang Sa basin to the southeast. Oceanic crust in the Xisha trough lies east of the map location. Water depth is in meters. Map generated by GeoMapApp [*Carbotte et al.*, 2004].

proposed to have occurred in response to Tibetan surface uplift [e.g., *Brookfield*, 1998; *Clark et al.*, 2004]. Unlike sedimentary basins onshore in east Asia the age control available from biostratigraphy in the marine sediments allows accurate age constraints to be placed on erosional and tectonic events. Moreover, because the vast majority of the eroded sediment lies in the offshore region a sediment budget for these areas is likely to be a robust proxy for changing continental erosion rates on eastern Tibet since the Eocene. Our goal is to use the marine stratigraphic record to understand how solid Earth tectonic activity, climate change and erosion interact in east Asia.

2. Geologic Setting

[4] The study area we examine here lies in the northwestern South China Sea between the island of Hainan and the coast of Vietnam (Figure 1). The basins overlap two tectonic provinces, with the Yinggehai basin lying within a transform zone at the southern end of the Red River fault zone. Opening of the NW-trending Yinggehai basin has often been linked to the southeastward slip and clockwise rotation of the Indochina block along the Red River fault zone [e.g., *Rangin et al.*, 1995; *Guo et al.*, 2001; *Sun et al.*, 2003, 2004]. Although the tectonic origin of the Yinggehai basin is debated [*Morley*, 2002], the NW-SE elongation of the basin, the location at the southern end of the Red River fault zone, and the steep faults that parallel the Red River fault and that bound the basin all argue that this basin is dominantly formed by deformation associated with the strike-slip tectonism.

[5] In contrast, the Qiongdongnan basin forms the western end of the rifted northern margin of the South China Sea, which was formed by rifting followed by seafloor

spreading along a WSW-ENE axis starting around 30 Ma in the northwestern area [*Taylor and Hayes*, 1980; *Lu et al.*, 1987; *Briais et al.*, 1993; *Yan et al.*, 2001; *Zhou et al.*, 2002]. Continental extension in the area is believed to have started in the Late Cretaceous-early Paleocene [*Ru et al.*, 1994; *Schlüter et al.*, 1996], and seems to have exploited the location of a preexisting Andean-type arc located above a north-dipping subduction zone along the southeast coast of China [*Jahn et al.*, 1976; *Hamilton*, 1979; *Sewell and Campbell*, 1997]. However, unlike the Pearl River Mouth basin, located between Hainan and Taiwan, the Hainan region lies to the northwest of the Cretaceous arc and instead overlaps a major Triassic "Indosinian" suture zone between southern China (Cathaysia) and Indochina that has been reactivated by the Red River fault zone during the Cenozoic [*Metcalfe*, 1996; *Lepvrier et al.*, 2004]. Despite this complex history there is no reason to suppose that the continental lithosphere under any of the regions studied here was significantly out of thermal equilibrium at the start of deformation. Indeed, *Clift et al.*'s [2002a] study of the South China Sea margins suggested that the lithosphere in the Hainan region was relatively rigid and cold compared to that under the Pearl River Mouth basin.

[6] The Qiongdongnan basin forms the western extension of the rifting that affected the Pearl River Mouth basin, but unlike that basin it does not directly juxtapose oceanic crust. *Briais et al.* [1993] placed the northwestern limit of seafloor spreading in the South China Sea just to the east of the study area shown in Figure 1. The deepwater basin, known variously as the Xisha, Hoang Sa or Paracel trough shows marine magnetic anomalies dating back to Anomaly 11 (~30 Ma), that define an original rift and spreading axis between Macclesfield Bank and the South China Shelf. Spreading subsequently jumped to a southerly position before propagating further toward the WSW [*Taylor and Hayes*, 1980; *Briais et al.*, 1993; *Zhou et al.*, 2002].

[7] The Yinggehai basin lies south of the Gulf of Tonkin, where *Rangin et al.* [1995] documented strike-slip deformation starting before 30 Ma and finishing at ~5.5 Ma. These authors argued for a major change in tectonic regime ~15 Ma because of a change in the sense of shear of the Red River fault zone, changing the basin from being transtensional to transpressional and linked to the cessation of seafloor spreading in the South China Sea at ~15 Ma. The northwestern Beibu Gulf was folded and inverted during the late Miocene, with inversion migrating toward the south and east, possibly in response to a southeastward movement of the South China block [*Sun et al.*, 2004].

[8] Onshore thermochronology work now constrains the age of motion on the Red River fault zone. A number of studies have used $^{40}Ar/^{39}Ar$ dating of metamorphic and granitic rocks in the Red River fault zone to constrain the start of motion to being before ~35 Ma [*Harrison et al.*, 1996; *Wang et al.*, 1998; *Leloup et al.*, 2001]. Most recently *Gilley et al.* [2003] used radiometric ages from high-temperature synkinematic garnets in metamorphic rocks from along the length of the Red River fault zone to constrain the onset of strike-slip motion as being close to 34 Ma.

[9] Although the Yinggehai and Qiongdongnan basins, as well as the continental Red River fault zone, do not appear to have been significantly active since ~5.5 Ma, Hainan Island itself and the nearby Leizhou Peninsula have been the locus of strong volcanism during the last 2 m.y., that appears to be linked to a deep-seated mantle seismic velocity anomaly [e.g., *Lebedev and Nolet*, 2003]. The geochemistry of the volcanic rocks on Hainan are not conclusive of tectonic setting but do support emplacement over hotter than normal, possibly plume-type mantle [*Tu et al.*, 1991; *Flower et al.*, 1998].

[10] It is still unclear what the driving mechanisms for the regional extension in the South China Sea are, although it has been suggested that extension was related to southward subduction under Borneo [e.g., *Holloway*, 1982; *Taylor and Hayes*, 1983; *Liu et al.*, 1985; *Hall*, 2002; *Morley*, 2002]. During the proposed subduction process, the southern margin of the South China Sea (i.e., Dangerous Grounds, Reed Bank, North Palawan Block) was suggested to have been displaced southward relative to mainland China and Indochina along a major N-S trending transform zone near the Vietnam margin. An alternative driving mechanism for extension favors southeastward lateral motion of Indochina and Borneo relative to a fixed China block [*Tapponnier et al.*, 1986; *Peltzer and Tapponnier*, 1988; *Replumaz and Tapponnier*, 2003]. A variety of radiometric dating and paleomagnetic studies have attempted to test this theory [e.g., *Packham*, 1996; *Burchfiel et al.*, 1997; *Wang et al.*, 1998; *Cung et al.*, 1998]. The timing of motion on the Red River fault does appear to be largely in accord with the timing of strongest, extension and seafloor spreading in the South China Sea [*Gilley et al.*, 2003]. However, many recent works indicate that the amount of offset during the time of South China Sea extension is insufficient to be the primary driving mechanism. As result the link between opening of the South China Sea and motion on the Red River fault system remains controversial [e.g., *Harrison et al.*, 1996; *Leloup et al.*, 1993, 2001].

3. Data Sources

[11] This study is based on a series of multichannel seismic profiles that cross and parallel the strike of both the Yinggehai and Qiongdongnan basins. These data were largely collected by BP Exploration plc in collaboration with the Chinese National Offshore Oil Company (CNOOC) in 1979 and 1980 (Figure 2). Though not of high density these lines do provide a regional overview of the structure and stratigraphy that is far in advance of anything now available in the open literature [*Fang et al.*, 2000; *He et al.*, 2002; *Rangin et al.*, 1995; *Wheeler*, 2000; *Gong and Li*, 1997, 2004]. Two newer lines (Profiles 3393 and 4540) were collected by CNOOC in 1991 and 1992 respectively and extend our coverage to the northwest, allowing the main depocenter of the Yinggehai basin to be examined. Age control is provided to the seismic stratigraphic through a number of drill sites, also shown in Figure 2. Because of the great sediment thickness there is no deep drilling in the central Yinggehai basin and consequently age control is limited for the oldest sedimentary rocks in that area. The presence of Eocene strata in the basin center is inferred on the basis of thin Eocene units drilled around the edge of the basin, and long-distance seismic stratigraphy. Age resolution is best for the Neogene strata because of the great number of wells that have penetrated

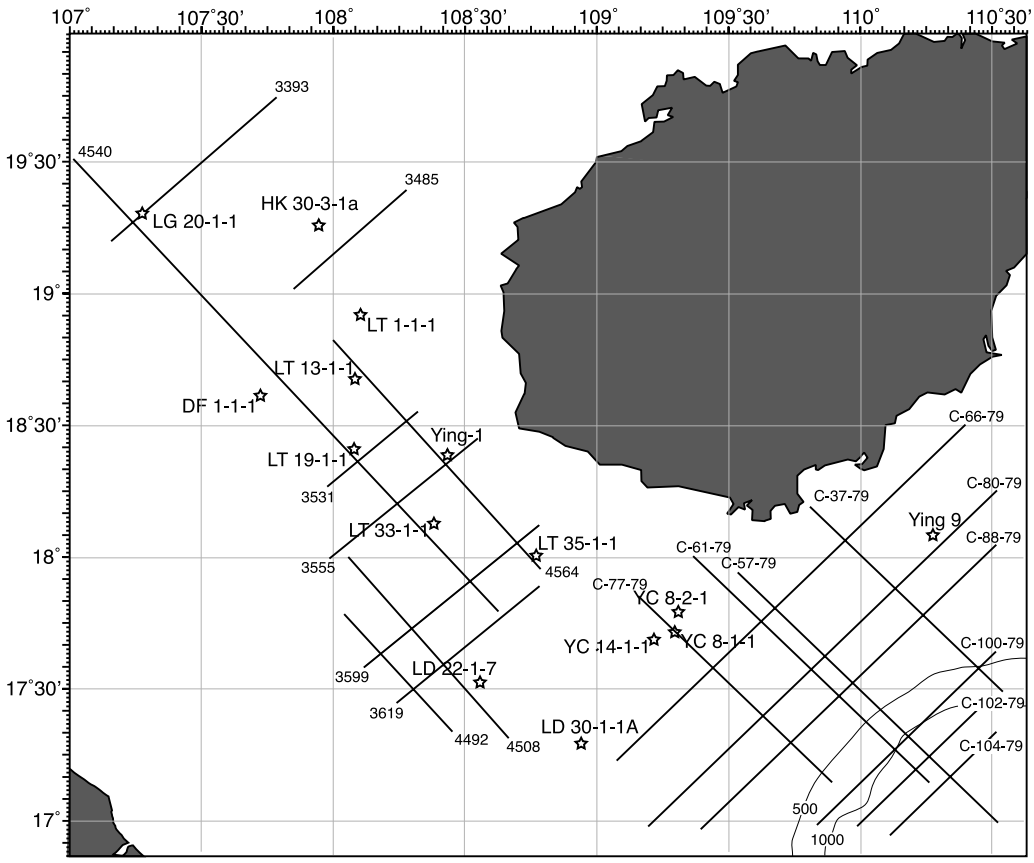

Figure 2. Chart showing the location of (solid lines) multichannel seismic profiles used in this study and (stars) the related wells that provide limited age control to the seismic stratigraphy. Thin contour lines show the 500 and 1000 m water depth contours taken from the GEBCO 2003 compilation [*British Oceanographic Data Centre*, 2003].

these formations, reflecting the fact that they are the main hydrocarbon reservoirs. Age control is provided by nannofossil biostratigraphy and is typical of the fairly low resolution used for industrial purposes, being limited to epoch and subepoch level [*Berggren et al.*, 1995]. Only in the Pliocene of the Yinggehai basin is greater resolution achieved, but this cannot be correlated with confidence into the Qiongdongnan basin. Dating of sequences was mostly done using cuttings rather than cored material, and while this can introduce a vertical uncertainty to the age picks (~10 m) this is generally small compared to the vertical resolution of the seismic data and the great thicknesses of the sedimentary packages themselves, so that is not considered to be a great source of error. Ages are converted from the biostratigraphic zone into numerical ages using the timescale of *Berggren et al.* [1995].

4. Seismic Stratigraphy

[12] Using the dating control and the seismic grids in the southern Hainan region it is possible to map out packages of sediment and reconstruct how the basins have filled and evolved through time. Figure 3 provides a large-scale regional image of the Yinggehai basin along the axis of the main depocenter, although the basement lies below the bottom of the recorded data in the center and is poorly defined along its northern edge. Nonetheless, it is possible to image the great sag that forms the basin center and note that it is not affected by major faulting through much of its stratigraphy. Large volumes of preserved Paleogene (mostly Oligocene) strata testify to vigorous subsidence at that time. Age controls indicate that the start of basement subsidence started after ~45 Ma, with a rapid acceleration in subsidence starting ~35 Ma [*Xie et al.*, 2001]. The stratigraphy shows that early and middle Miocene subsidence was also strongly focused close to the basin center (near intersections with Lines 3531 and 3555) after being stronger further north in the Oligocene (near intersections with Line 3393). At the northern end of the basin there is a pronounced thinning of the 16–21 Ma sediment package after a thick older sequence, suggesting inversion and uplift in this area after 21 Ma. However, further south it is apparent that the middle Miocene (13.8–11 Ma) thins rapidly toward the south on to a structural high that did not influence the stratigraphic thicknesses of the lower Miocene, and which must have been generated by later tectonism. Inversion appears to be diachronous within the basin; older in the north, younger in the south.

[13] The middle Miocene is the youngest stratigraphic unit to show clear, high-amplitude folding (especially near the intersections of Line 4540 with Lines 3531 and 3555; see Figure 3), suggestive of basin inversion prior to the end of the early middle Miocene at 13.8 Ma. The upper Miocene also shows ponding and thinning against the structural high

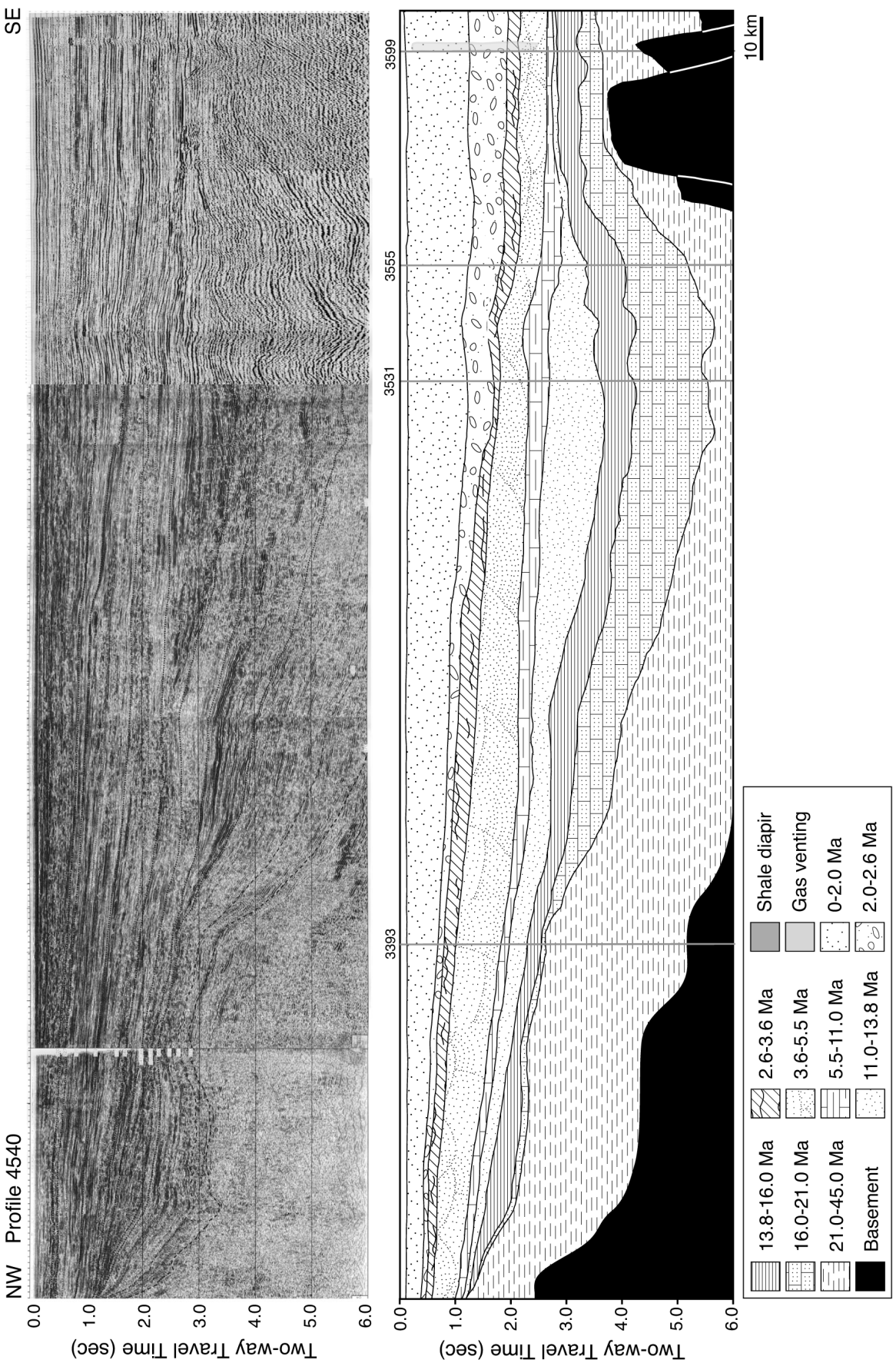

Figure 3. Seismic section and interpretation of Profile 4540 running through the center of the Yinggehai basin. Basement is not well imaged in this line and is below the bottom of the recorded data in the basin center. Note how the depocenter migrates to the southeast in the Pliocene after being over the region of maximum basement subsidence for much of the Neogene. Location is shown in Figure 2.

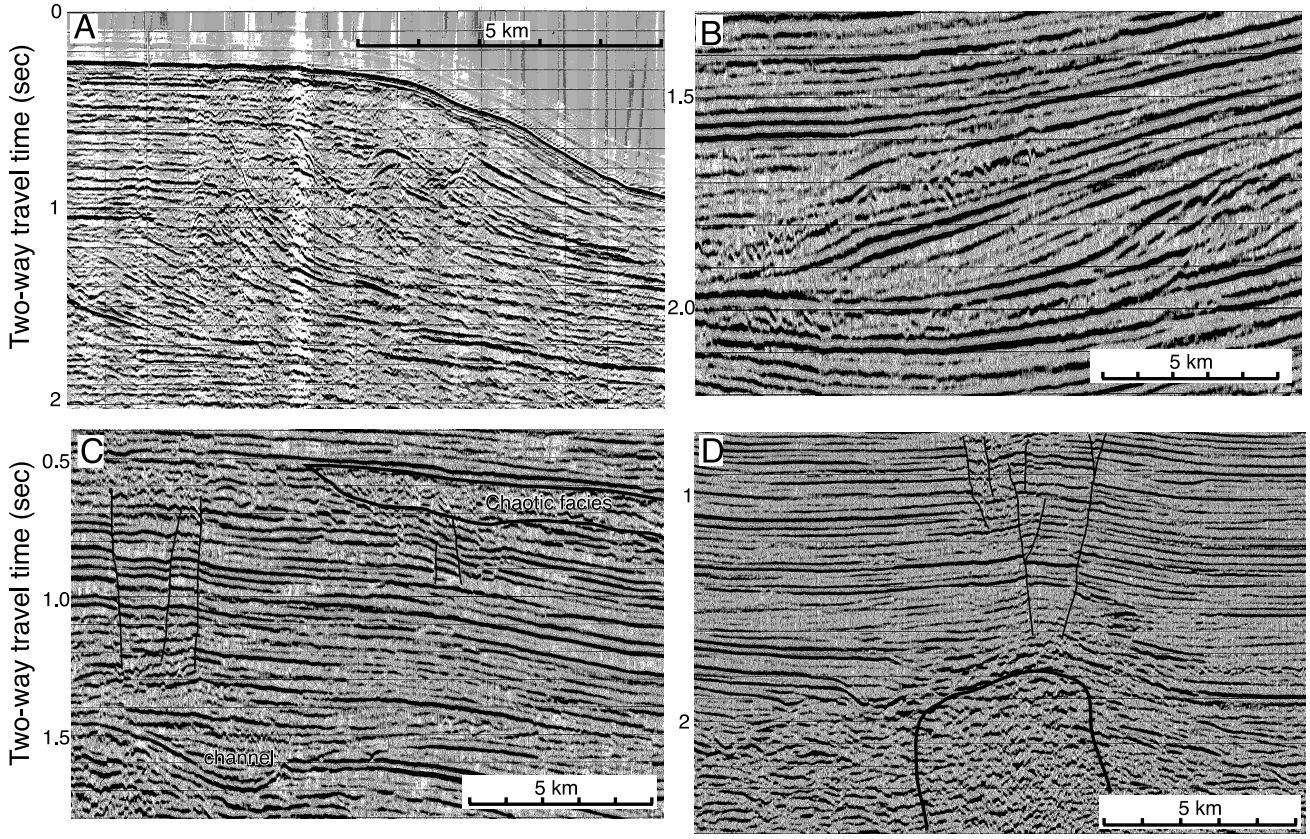

Figure 4. Examples of seismic features seen offshore Hainan. (a) Plio-Pleistocene prograding foresets forming the shelf edge in the Qiongdongnan basin, SW Hainan, Line C-57-79. (b) Prograding deltaic foresets in upper Pliocene sediments in the eastern Yinggehai basin, Profile 3599. (c) Erosive channel overlain by parallel-bedded sandy strata, affected by small-scale faulting on left side of section. Debris flow units are seen interbedded in upper right side of section; eastern Yinggehai basin, Profile 3599. (d) Small-scale faulting above a shale diapir in central Yinggehai basin, Line 3619.

at the southern end of the Yinggehai depocenter, but the upper Miocene depocenter is displaced south compared to that of the upper middle Miocene. The Plio-Pleistocene continues this south-migrating trend and eventually shows simple thickening to the south along Profile 4540. The strong 5.5 Ma unconformity noted by *Rangin et al.* [1995] in the northern Gulf of Tonkin region is not so clear in the southern Yinggehai basin. There is no major erosion surface or structural inversion of that age seen in Figure 3 or any other profile considered in this study.

4.1. Seismic Facies

[14] Figure 4 shows some of the seismic features that characterize the sections analyzed in this study. Large-scale, southward-prograding and aggrading foresets are a characteristic feature of the Plio-Pleistocene in the Qiongdongnan basin (Figure 4a), but are less well developed in the Yinggehai basin at this time. However, Pliocene foresets are found in the Yinggehai basin prograding mostly westward, but also to the NW and SW away from Hainan, and indicative of mass flux from the island at this time. There is no evidence for major sediment flux from the direction of Vietnam into the central or eastern Yinggehai basin. Figure 4b shows an example of the Pliocene foresets in the Yinggehai basin. These features are generally not well developed at deeper stratigraphic levels. In addition to foresets, the seismic data reveal a series of smaller-scale facies. While most of the units show parallel-bedded reflectors, Figure 4c shows a series of other features that are recognized locally, including channelized erosive surfaces and poorly bedded chaotic facies that often form lens-shaped deposits mantled by better-bedded units. We interpret these bodies as debris flow deposits. In addition, small-scale faulting can be seen frequently in the section, even in shallow, Plio-Pleistocene units (Figure 4c). Faulting is especially well developed over the crests of the shale diapirs observed in the basin center [*Hao et al.*, 2000; *Xie et al.*, 1999, 2003] (Figure 4d). While most of the large-scale faulting is restricted to the basement and the Paleogene sedimentary rocks, seismic evidence from the eastern margin of the basin clearly shows major transtensional faulting cutting high into the section (Figure 5), testifying to tectonism in the basin well into the Pliocene.

[15] Figure 6 presents a section cutting across the strike of the Yinggehai basin and showing the steep basin margin that drops off sharply into the Yinggehai depocenter. In this southeastern part of the Yinggehai basin the deformation appears to be spread across several faults that step down into basin center, although with the greatest throw on the strand closest to Hainan, called number one fault in the

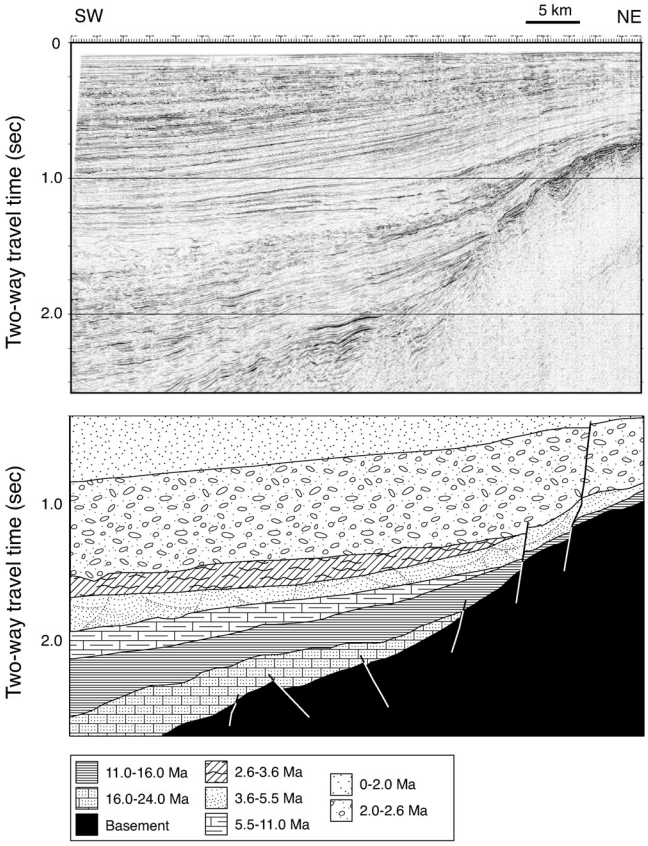

Figure 5. Multichannel seismic Profile 3485 located offshore NW Hainan Island on the eastern margin of the Yinggehai basin. (top) Original data; (bottom) interpretation. Note that while faulting mostly affected the basement and oldest sediments, there is clear reactivation of the faulting along the northeastern end of the line, where Pliocene strata are cut. Location is shown in Figure 2.

Chinese literature. Further north the basin boundary is sharper again (Figure 7), emphasizing the dominant influence of the number one fault and the strike-slip character of the tectonism that created most of the accomodation space. In both sections the oldest sediments are restricted to the deeper part of the basin, though the upper middle Miocene clearly onlaps on to the most landward structural high. Not surprisingly there is a general thickening of strata westward into the basin center.

[16] Lack of corresponding data from the western, Vietnamese part of the basin precludes us from defining the structure of the western margin at this time, although it is not as steep as the eastern boundary. The slight thinning of sediment toward the southwestern end of Profile 3599 indicates that our profiles do cover the main depocenter (Figure 6). Figure 6 also clearly shows a major deep-rooted shale diapir located near the basin center that cuts upsection into the Pliocene. The source of the diapir is in the Paleogene strata, although the data do not allow that level to be very well defined. Three more diapirs are seen on Profile 4508 (Figure 8), running through the center of the Yinggehai basin. The diapirs do not reach the modern seafloor, although one penetrates as high in the stratigraphy as the Pleistocene. Like Profile 4540 (Figure 2) that also runs along the basin axis, Profile 4508 shows a clear, low-amplitude folding of the lower parts of the stratigraphy, indicating a compressional phase during basin filling.

4.2. Shale Diapirism

[17] Figure 9 shows a close-up of the central diapir structure on Profile 4508 that allows its evolution to be seen more clearly. The diapir seems to cut vertically through the older strata but above the level of the 2.6 Ma reflector the diapir has ''wings'' that appear to prograde on to adjacent reflectors, giving the impression of a mud volcano on the paleoseafloor. The same type of relationship is also seen in the most northeasterly diapir. The Pliocene was clearly the most active time for shale diapirism because even the deeper buried diapir in Figure 8 shows channelized and uplifted reflectors in the Pliocene strata above the diapir, indicating seafloor doming at that time. The central diapir shown in Figure 9 seems to have developed into a sink after its initial eruption and formed a basin that new sediment draped over well during the Pleistocene. About half way through the Pleistocene the depression appears to decrease in depth and is progressively infilled and buried, indicating a cessation of activity. The most intense phase of shale diapirism appears to be bracketed by the 2.0 Ma and 2.6 Ma reflectors.

4.3. Qiongdongnan Margin

[18] The stratigraphy of the Qiongdongnan basin is shown in Figure 10, where the dominance of the giant Pliocene foresets in defining that margin's stratigraphy is apparent. Compared to the Yinggehai basin the Miocene is relatively poorly developed, although there are significant thicknesses of Paleogene. Faulting of the basement is better defined by seismic data here because of the reduced overburden and clear imaging of the sediment-basement contact. The basement structure appears to be dominated by a series of tilted fault blocks with no evidence for significant volcanism related to rifting. The contrast with the Yinggehai basin structure is marked because the strain is partitioned across many smaller faults, rather than one major structure. Fault reactivation does appear to affect the Paleogene and maybe the lower Miocene, although the amount of offset is small compared to that along the top basement surface. Rifting appears to be largely complete prior to 24 Ma.

5. Estimating Sediment Volumes

5.1. Time-Depth Conversion

[19] In order to reconstruct the basin sedimentary budget and calculate tectonic subsidence rates it is first necessary to convert the vertical scale of the seismic profiles from time into depth measured in meters. This was done largely through the use of the stacking velocity data that were generated during the original processing of the multichannel reflection data. Interval velocities were calculated and are shown in Figure 11 plotted against depth for Profiles 3599 and 4508 in the Yinggehai basin and C-57-79 in the Qiongdongnan basin, although the same process was repeated for all of the profiles considered here. Not surprisingly seismic velocities typically increase with depth, but increase less rapidly where the sediment pile is thickest.

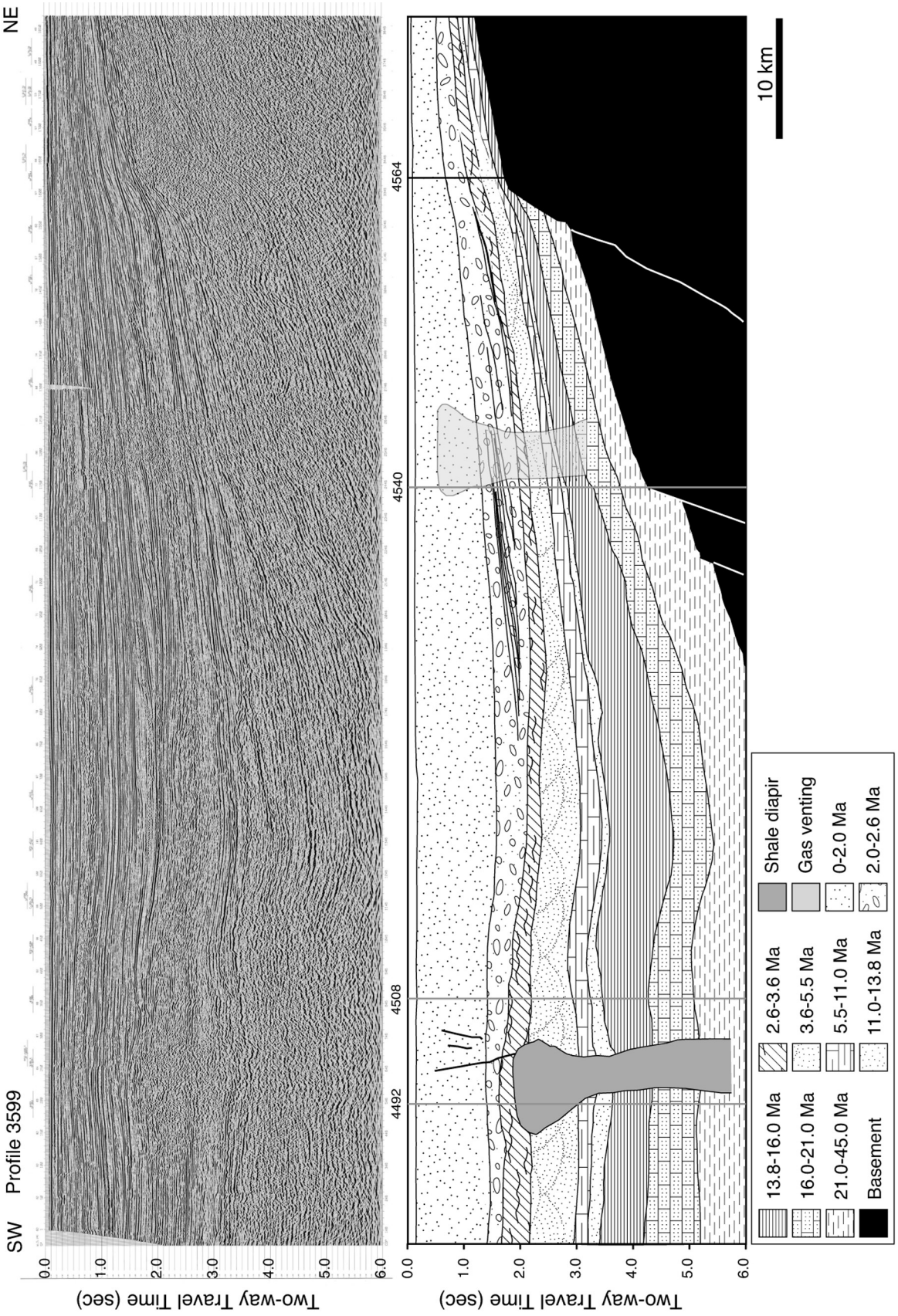

Figure 6. Multichannel seismic Profile 3599. (top) Original data; (bottom) interpretation. Section shows the sharp eastern boundary to the Yinggehai basin controlled by the number one fault and associated strike-slip splays. The depth to basement in the basin center is not controlled by this section. Location is shown in Figure 2.

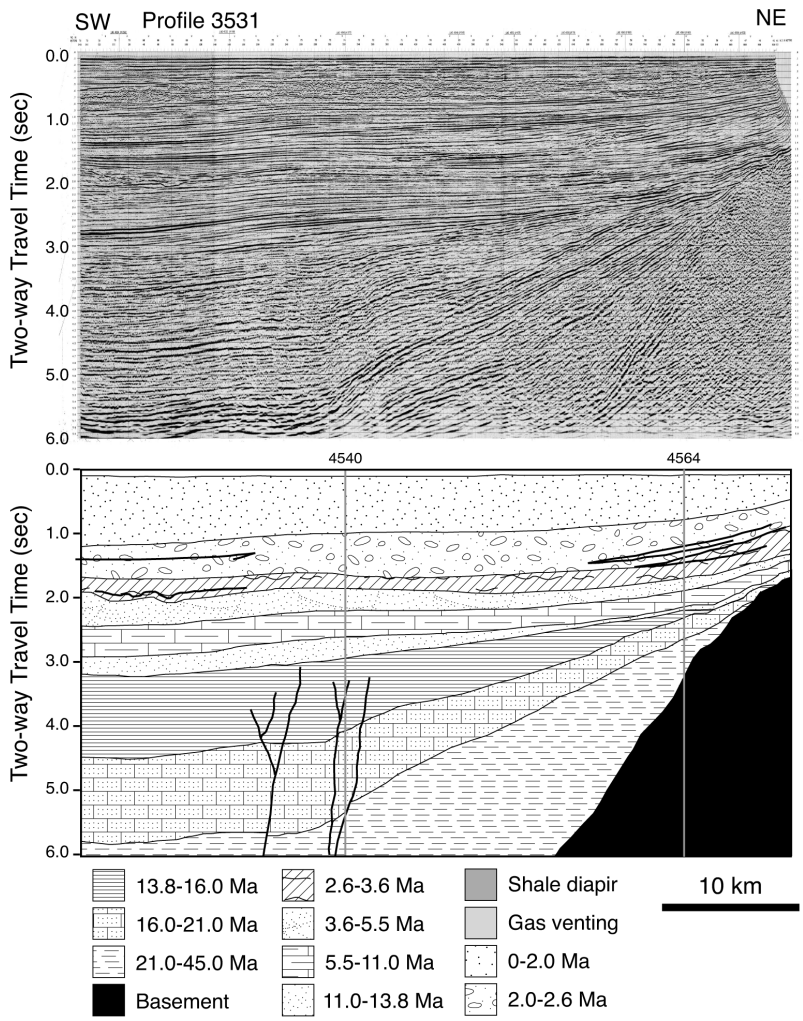

Figure 7. Multichannel seismic Profile 3531. (top) Original data; (bottom) interpretation. Section shows the sharp eastern boundary to the Yinggehai basin controlled by the number one fault, emphasizing the strike-slip dominance of the basin tectonics. Location is shown in Figure 2.

[20] It is noteworthy that there are significant areas where there are velocity inversions, most especially in the central Yinggehai basin. The presence of velocity inversions is suggestive of uncompacted, overpressured sediments at depths of 2–6 km. These regions broadly correlate with the zones of shale diapirism, although the inversions are more pronounced at the southeast end of Profile 4508, away from the largest diapirs at the northwest end. As noted in section 4.2, these diapirs are no longer active, so the lack of direct correspondence is not anomalous, but it does indicate that there are still excess pore pressures at depth in the Yinggehai basin, especially at the southern end of the basin, where the youngest sedimentation has been most rapid. There is limited evidence for velocity inversion and overpressuring under the shelf edge of the Qiongdongnan basin, but to a much lesser extent than seen in the Yinggehai basin.

[21] Once the velocity structure of each profile was determined it was possible to convert the stratigraphy to depth sections, as shown in Figure 12. Once in this state then it is relatively straightforward to map out sediment thicknesses and perform backstripping calculations. As a first step the depth conversion allows total sediment thicknesses to be described. Figure 13 shows a basin-wide isopach map for the entire Yinggehai–Song Hong region, based partly on the data presented here, partly on gravity and drilling data, and partly on confidential seismic data from both the Chinese and Vietnamese parts of the basin [*Hao et al.*, 1995; *Gong and Li*, 1997, 2004]. Sediment thicknesses are estimated at around 17 km in the depocenter, making the Yinggehai basin one of the thickest sediment accumulation on Earth. The steep character of the basin's eastern margin is again apparent in this depth-converted plot, controlled largely by the "number one fault." On the western side of the basin there is a more gradual slope caused by the interaction of several splayed transform faults, though all broadly related to the Red River fault zone. The basin depocenter itself is divided into three subcompartments by uplifted basement regions, as seen in Figure 3. It is noteworthy how little of the sediment mass lies onshore under northern Vietnam, even though the drilled sediment thicknesses in the Hanoi basin exceed 5 km. The isopach map emphasizes the need to estimate the sediment budget offshore if any serious attempt is to be

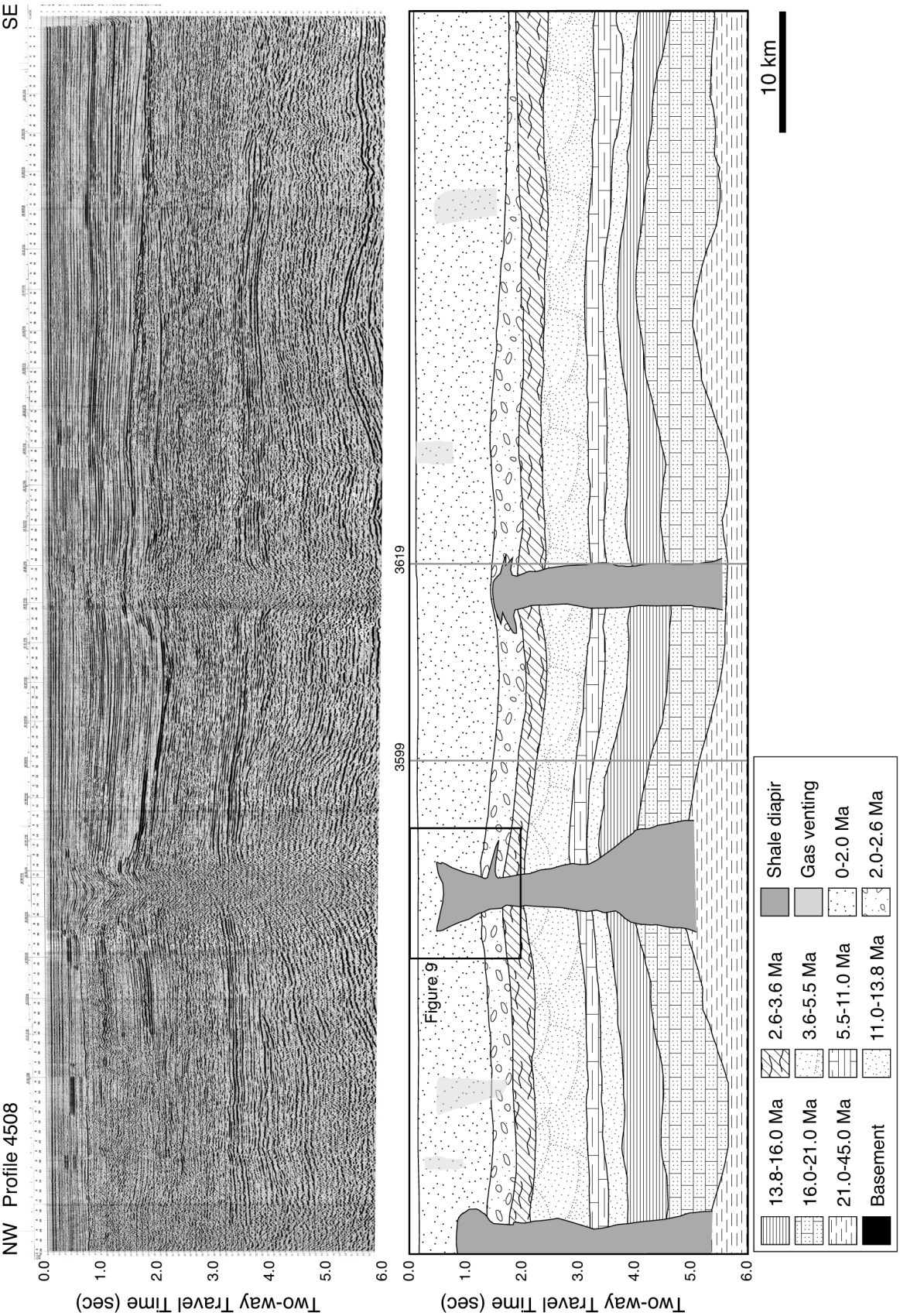

Figure 8. Multichannel seismic Profile 4508. (top) Original data; (bottom) interpretation. This profile images the deepest part of the Yinggehai basin and shows the presence of three deep-seated shale diapirs as well as common areas of gas venting. Note folding of strata affecting the Paleogene most strongly but also up to the Pliocene. Location is shown in Figure 2.

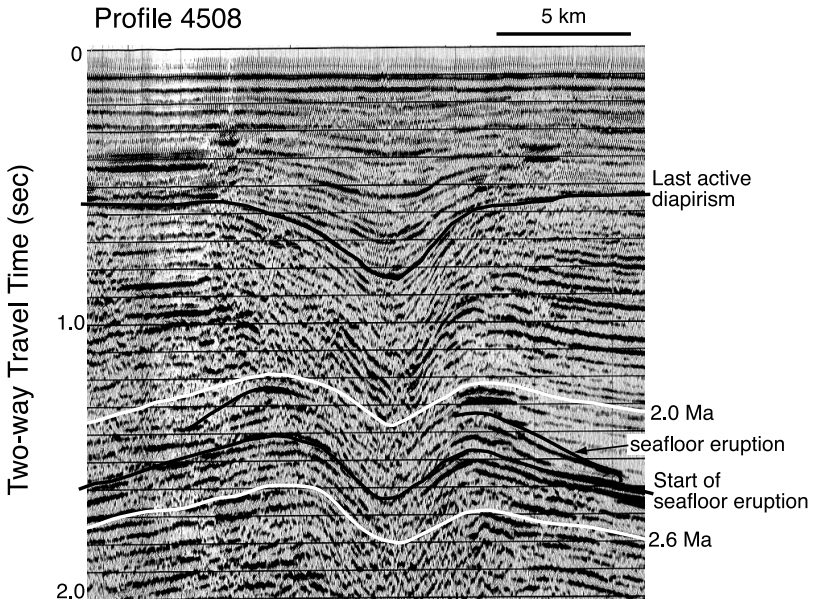

Figure 9. Close-up of shale diapir from Profile 4508 in the central Yinggehai basin showing the best developed vertical disruption of reflectors, the dipping reflectors interpreted as seafloor mud eruptions, and the infilling of the collapsed pipe during the Pleistocene after the end of activity.

made in quantify the erosion history in the Red River drainage.

5.2. Structural and Stratigraphic Mapping

[22] The newly presented network of seismic profiles in the Qiongdongnan and southern Yinggehai basins now allow us to map in detail the structural relationships between the basins and the evolution of the sedimentary fill. Figure 14 shows the distribution of major faults cutting the prerift basement in the southern Hainan region. The change in orientation between the two sets of faults is striking, with a clear sense that the Yinggehai strike-slip faults crosscut those of the extensional Qiongdongnan basin. This makes structural sense, because the seismic data indicated a cessation of major extensional faulting in the Qiongdongnan basin prior to 24 Ma, yet strike-slip faulting in the Yinggehai continued at least until structural inversion prior to 13.8 Ma. Figure 14 emphasizes the importance of the number one fault in controlling the tectonics of the eastern margin of the Yinggehai basin, confirming a dominant strike-slip mechanism for basin formation. The pattern of faulting is consistent with analogue modelling of *Sun et al.* [2004] in which the fault patterns of the Hainan region were duplicated by NNW-SSE directed extension between Hainan and the Xisha Block, coupled with a clockwise rotation and SSE motion of Indochina. In addition, Figure 14 maps out those shale diapirs that are cut by the seismic profiles analyzed here, as well as gas escape chimneys. As noted by *Xie et al.* [2003] these features can be readily mistaken for one another, not least because both are associated with the deeper part of the Yinggehai basin. The largest gas chimney is found close to one of the major bounding faults, consistent with a structural control on fluid escape [*Xie et al.*, 2003]. In this study we distinguished shale diapirism through identification of actual deformation of the surrounding strata rather than a simple vertical column of poorly imaged reflectors.

[23] Depth conversion allows the broad-scale stratigraphic evolution of the margin to be mapped out. As seen in Figure 3, much of the Oligocene and especially early Miocene sedimentation was focused in the center of the Yinggehai basin, so here we look at the later evolution, which is also better defined by seismic data and constrained in age by drilling. *Sun et al.* [2004] noted the general temporal migration of depocenters to the south, a conclusion confirmed by this work. Figure 15c shows that the middle Miocene is most thickly developed in the central Yinggehai basin, exceeding 4 km, but thins rapidly into the Qiongdongnan basin. A similar pattern is noted in the upper Miocene, though with a moderate shift in depocenter to the south. However, it is in the Plio-Pleistocene that the greatest change is noted, with the thickest deposits found in the Qiongdongnan basin. Nonetheless, locally more than 2 km of Plio-Pleistocene can still be found in the Yinggehai basin.

[24] Given the modern shallow water depths and the drilling evidence for long-term shallow marine conditions during the Neogene it seems likely that the southward migration of the depocenter reflects the loss of accommodation space in the Yinggehai basin due to the slowing or even inversion of tectonic subsidence, coupled with large volume of sediment influx, as shown by the foresets seen in these sedimentary units sourced from Hainan.

5.3. Estimating Sedimentary Budgets

[25] We here estimate the changing sedimentary flux into the Red River offshore region using a standard array of basin analytical tools, but largely on the basis of two-dimensional backstripping of depth-converted seismic profiles. The approach is simple and is based on restoring each section to its state immediately after the end of deposition of

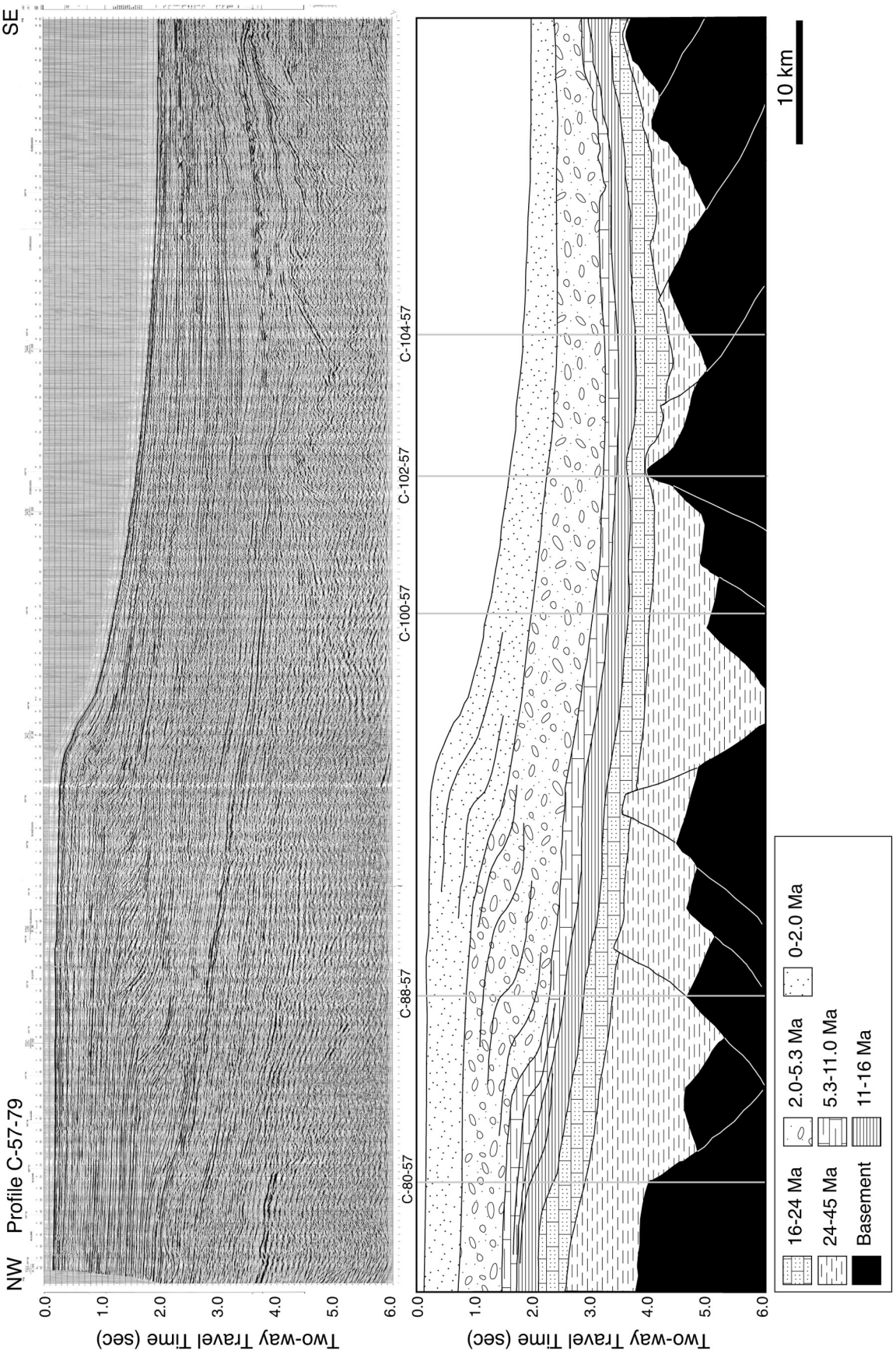

Figure 10. Multichannel seismic Profile C-57-79. (top) Original data; (bottom) interpretation. This profile shows many of the features typical of the south Hainan margin and the Qiongdongnan basin. Basement structure is typical tilted fault block style, while the sedimentary cover is dominated by thick, mostly Plio-Pleistocene foresets, migrating south into deep water. Location is shown in Figure 2.

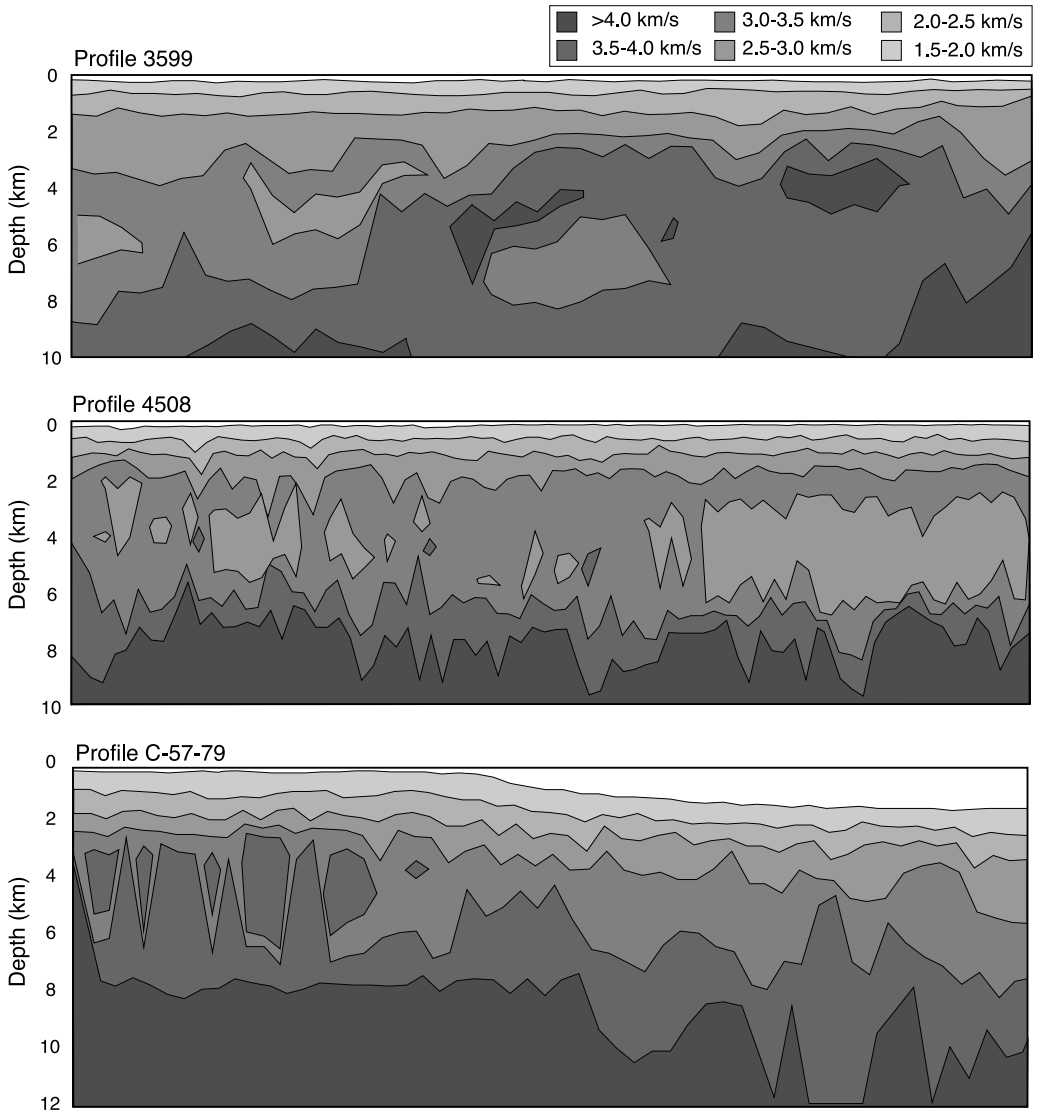

Figure 11. Plots of seismic velocity versus depth for three of the seismic sections interpreted in this study. The velocities are derived from the stacking velocities calculated during processing of the multichannel seismic reflection data. Locations of each line are shown in Figure 2.

each dated sedimentary package. By determining the volume of sediment deposited between each dated reflector we can determine rates of accumulation by dividing the sediment volume by the duration of each depositional episode. The restoration of the basin to its former states is done by following the approach of *Sclater and Christie* [1980] in which the stratigraphy from each successive dated sediment package is unloaded and decompacted. Here we use the program Flex-Decomp™ [*Kusznir et al.*, 1995] to restore the original, preburial thickness. By so doing we are able to compare deposited volumes at different time periods before compaction, which if unaccounted for would result in an apparent and unrealistic reduction in sedimentation rate in deeply buried (i.e., compacted) stratigraphic units.

[26] The degree of burial compaction varies with lithology. We use the lithologies and porosities sampled by drilling, supplemented by average rates of burial compaction derived from numerous industrial wells where local data do not exist [*Sclater and Christie*, 1980] to correct for compaction and to estimate sediment volumes deposited during each time period. Until a high-resolution timescale can be provided by continuously cored scientific boreholes the age resolution of our reconstructed accumulation rate model is constrained by the relatively broad-scale time divisions derived from the age picks in the petroleum exploration wells. As each section is unloaded and decompacted we add the budgets together in order to derive a basin-wide budget. A simple addition and normalization procedure gives more weight to the longest lines, which is reasonable because they represent more of the basin fill. Basin-wide rates of sediment accumulation are then calculated using the normalized rates for each dated interval and an estimate of the total basin volume.

[27] For the large time periods considered here the major uncertainties in the backstripping process are caused by variations in the seismic velocity and in the deviation of sediments from a typical compaction history. The former is by far the largest uncertainty, and we estimate that errors

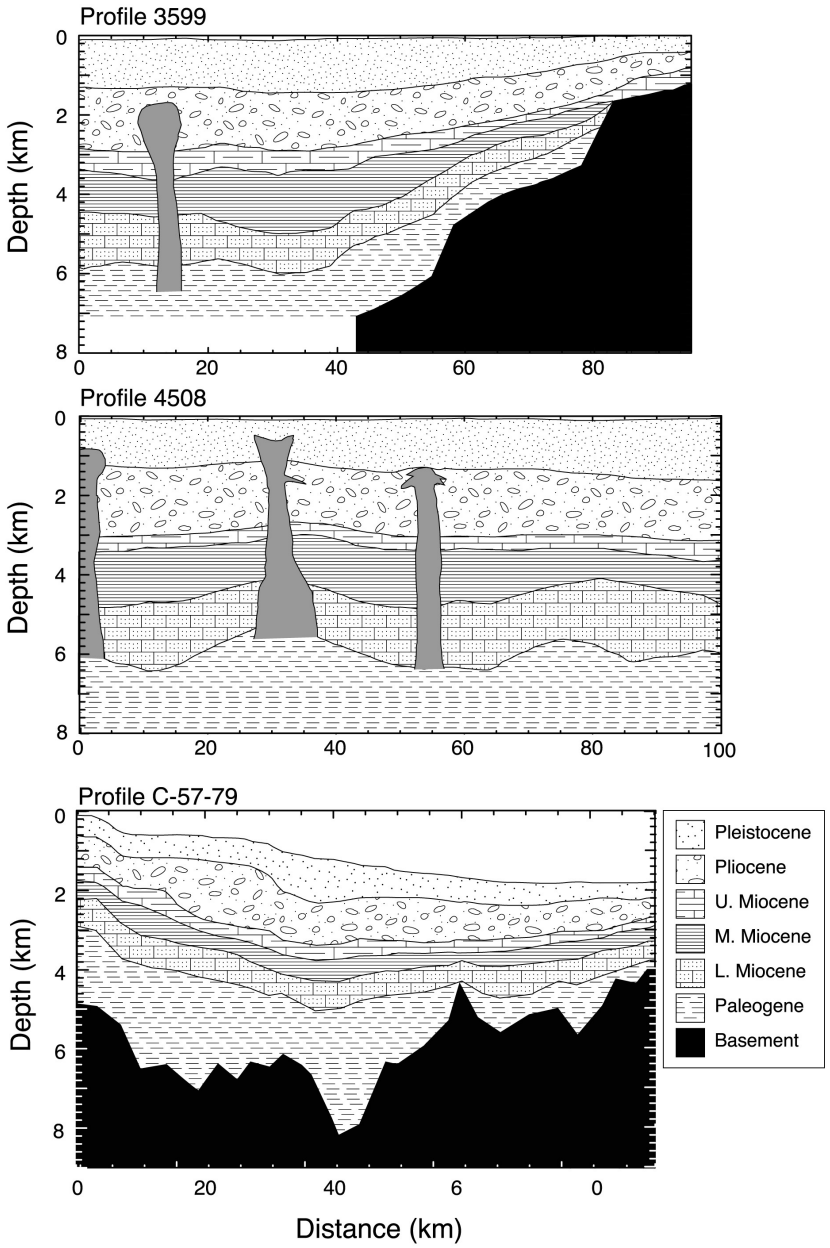

Figure 12. Geological cross sections from Profiles 3599, 4508, and C-57-79 showing the structure and stratigraphy after conversion of the vertical axis from time to depth, using the velocity structures shown in Figure 11.

could rise as high as 20%, given the lateral variability in the stacking velocities and their poor resolution in the deeper parts of the basin (>5 km). Overpressuring, for which we have ample evidence in the upper mid-Miocene can affect passive margin sequences where sedimentation is rapid [e.g., *Burrus*, 1998]. The shale diapirism recognized in the deepest sections of the Yinggehai basin [*Xie et al.*, 1999; *Fang et al.*, 2000] shows the effect of overpressuring during Pliocene times, while the velocity inversions seen locally in Figure 11 allow a correction to be made, on the basis of the magnitude of the velocity anomaly. Compared to the potential errors in the velocity-depth conversion this influence is relatively small.

[28] In this study we have constructed two independent sediment budgets for the Qiongdongnan and Yinggehai basins (Figure 16). Not surprisingly these are quite different from one another, although they both share the swift increase in rates after 5.5 Ma, as might be anticipated from the well-developed foresets seen on seismic of this age. The better age resolution of the Yinggehai profiles picks out the period of 2.6–2.0 Ma as being a time of especially fast accumulation.

[29] The major difference between the Qiongdongnan and Yinggehai basins is that the Yinggehai shows a large peak in the early and middle Miocene rates, which were still slow in the Qiongdongnan basin. This likely reflects the dominant source of sediment being from the north (i.e., the Red River) and the sediment being mostly captured by the fast subsiding Yinggehai basin at that time, thus preventing overspill into the Qiongdongnan basin. The situation in the Pliocene

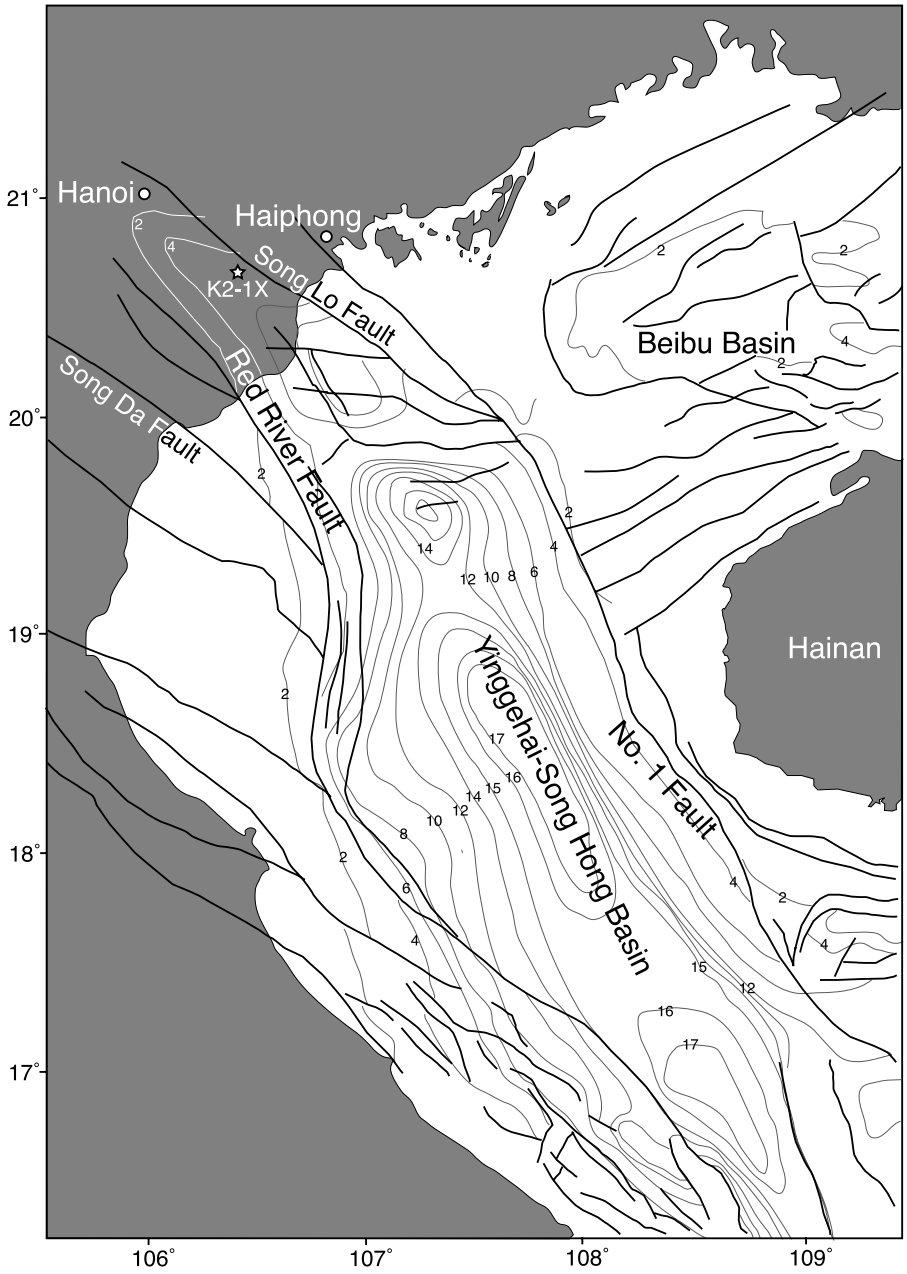

Figure 13. Total sediment isopach map for the Yinggehai–Song Hong basin on the basis of the interpretation of profiles shown in Figure 2 and classified data from the Chinese National Offshore Oil Company and PetroVietnam combined with gravity data. Note sediment thickness estimated ~20 km in the basin center.

differed because sediment supply outstripped the tectonic subsidence in the Yinggehai basin, allowing overspill of Red River–derived sediment to the south, and because uplift of Hainan at that time was feeding some sediment directly into the Qiongdongnan basin. There is no suggestion that erosion from the coast of Vietnam south of the Red River delta was a significant source of sediment to those parts of the basin considered here.

[30] Figure 16 also shows a synthesized sediment budget for the entire Red River system, including the Hanoi basin onshore. In practice this represents the combination of our extensive new data from the central and southern Yinggehai regions with the previously published budget of *Clift et al.* [2004] that was based on seven profiles, several from the northern Yinggehai–Song Hong region and one from the Beibu Gulf. Although the different seismic profiles have different and sometimes superior age controls compared to our study, the overall pattern of the sediment flux is quite similar to that we have derived from this new data, albeit with a better defined gradual increase in rates during the Paleogene. Our resultant budget is more representative than that published by *Clift et al.* [2004] because of the better

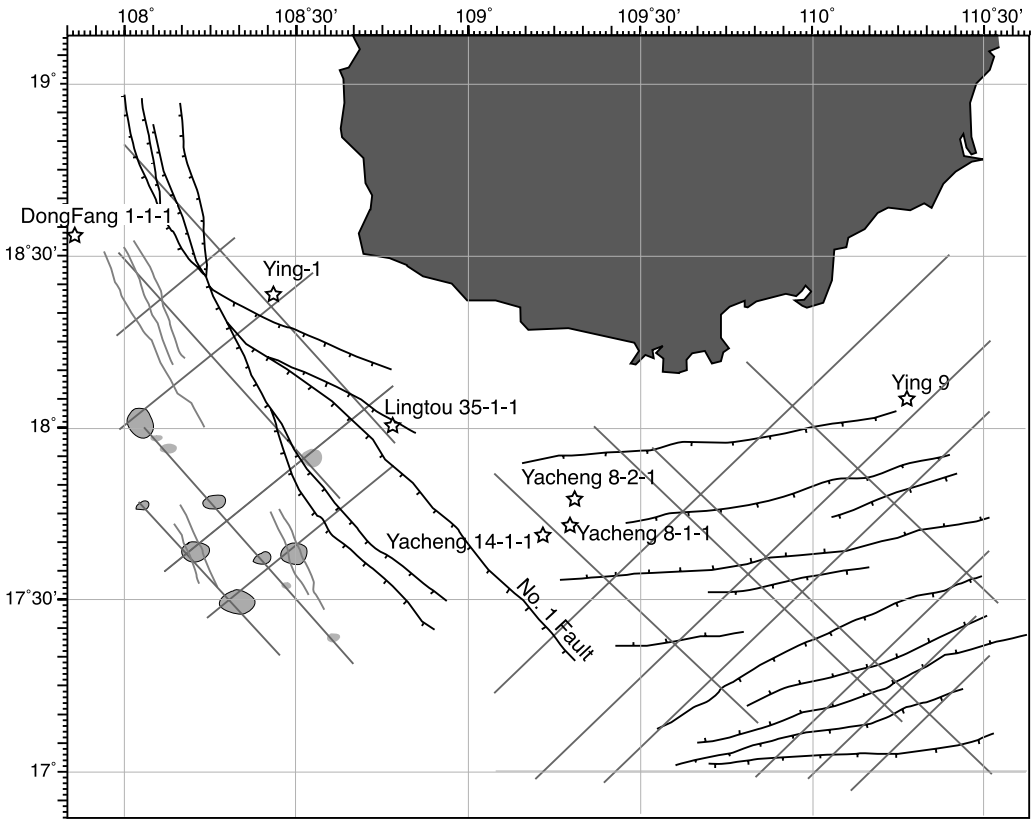

Figure 14. Map of the southern Yinggehai and Qiongdongnan basin region showing the major faults identified on the seismic profiles shown in Figure 2. Interpreted profiles are shown as gray lines and faults are shown as black lines with tick marks indicating the downthrown side. Dark gray shaded shapes with solid outlines in the western region indicate individual shale diapirs identified in this study. Light gray shaded shapes with no solid outline indicate areas of major gas venting.

coverage for the central regions of the basin, which represent main depocenter.

6. One-Dimensional Tectonic Subsidence Analysis

[31] As well as allowing sediment accumulation rates to be calculated, the unloading and decompaction of the sedimentary fill allows the tectonic subsidence of the basement to be assessed if water depths of deposition can be estimated. This is hard to do in the Qiongdongnan region because of the continuing great water depths in the basin center, and the difficulty in getting good paleowater depth estimates from deepwater sediments, even if core is available, which it typically is not. The Yinggehai basin, however, is thought to be dominantly infilled by shallow marine and deltaic sediments that limit water depths to 0–50 m through much of the stratigraphy. Observations from the modern Hanoi basin indicate that even subaerial, fluvial units are not thought to be deposited more than 10 m above sea level. As a result we have relatively tightly controlled subsidence reconstructions for the Yinggehai basin because these uncertainties are small compared to the total amount of subsidence.

[32] We employed the method of *Sclater and Christie* [1980] at six relatively well dated and complete drilled sections that span several different parts of the basin, including the Hanoi trough. The objective was to isolate and quantify the residual subsidence history of the basement, after correcting for the loading effect of the sedimentary overburden so that we might date and quantify different stages of the basin formation process. Backstripping makes no assumption about the tectonic mechanism causing basement subsidence and can be equally applied to strike slip and extensional basin. The backstripping process necessarily involves assuming local isostatic compensation, which is close to being accurate in the South China region, where synrift effective elastic thickness (Te) has been estimated at 1–3 km in the Pearl River Mouth basin [*Bellingham and White*, 2000; *Clift et al.*, 2002b]. Gravity data indicate that Te should not be much more in the study region [*Braitenberg et al.*, 2002]. The input data were lithology, age, and paleowater depth, all of which were estimated by CNOOC, PetroVietnam and BP contractors and were recorded on standard oil industry well logs. There is no reason to suppose that the quality of these data is poor, although these data cannot be readily verified. Each log provides an array of foraminifer and nannofossil, and sometimes palynological biostratigraphic data and was converted to a numerical age using the scheme of *Berggren et al.* [1995].

[33] The unloading and decompaction process was described in section 5.3; however, in the case of a basement subsidence analysis the section is also restored to its original water depth of deposition in order to estimate the depth to basement for each dated horizon. Correction can also be made for the fluctuations in the global eustatic sea level. In this work the second-order sea level reconstruction of *Haq et al.* [1987] was used, despite controversy related to the

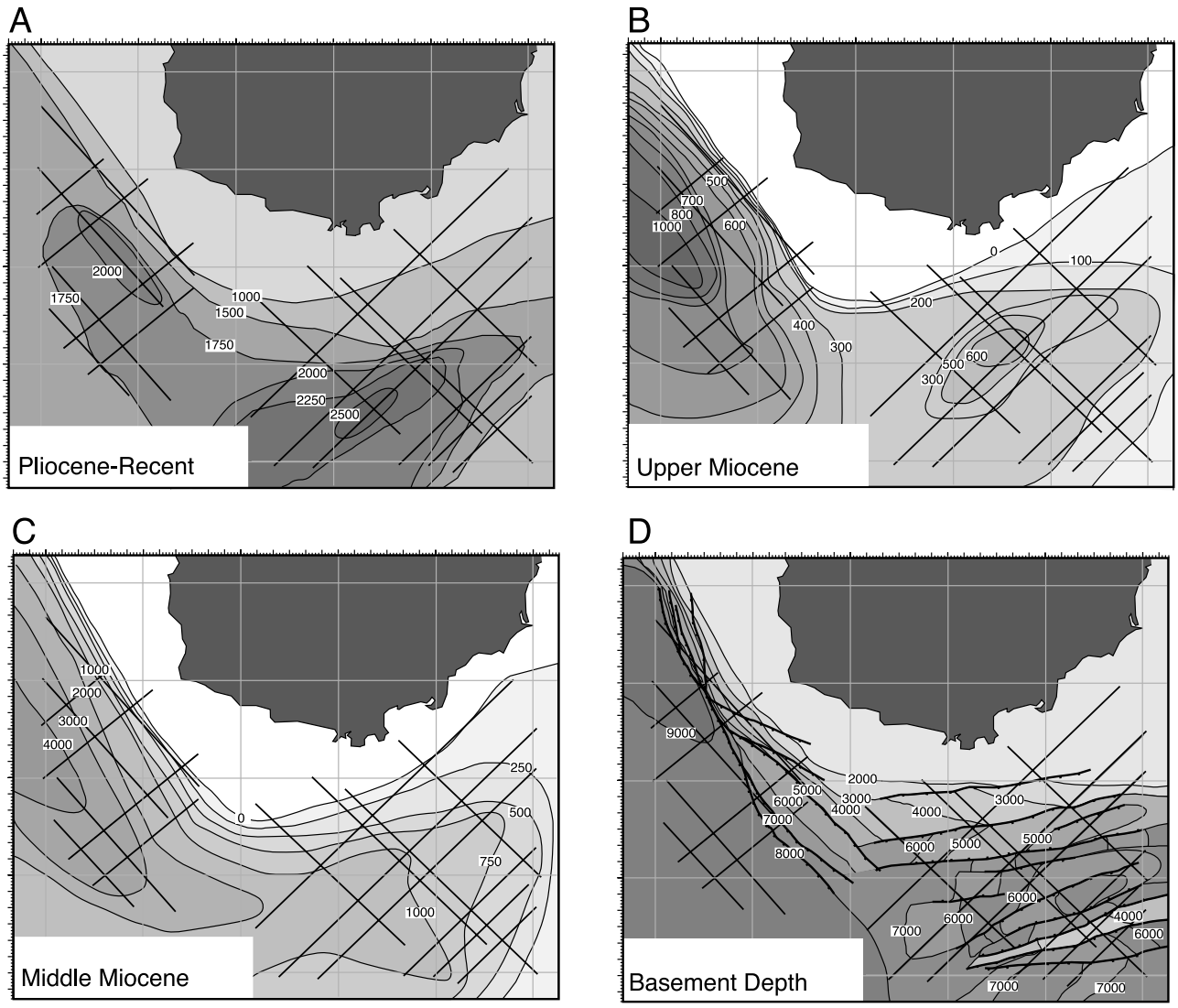

Figure 15. Isopach maps of some of the major stratigraphic units in the southern Yinggehai and Qiongdongnan basin region. (a) Pliocene-Recent, (b) upper Miocene, (c) middle Miocene, and (d) depth to top of acoustic prerift basement. Note southerly migration of depocenter into the Qiongdongnan basin during the Pliocene. Strata unit thicknesses are in meters.

timing and especially magnitude of sea level fluctuations. Sea level variability determined from paleoceanographic isotopic studies [e.g., *Miller et al.*, 1987] is only about one third of the magnitude estimated from sequence stratigraphy by *Haq et al.* [1987]. Consequently our reconstruction may overestimate the influence of falling sea levels, which would result in overestimates of the amount of tectonic subsidence. The net effect of using the *Haq et al.* [1987] sea level correction is to increase total subsidence and thus estimates of lithospheric extension, although the size of the sea level correction is modest compared to the basement subsidence (<10% in most cases).

[34] The result of these calculations is a reconstruction of the depth to basement through time as if the basin had only been filled with water (Figure 17). The results from the southern and central Yinggehai basin show long-term subsidence, with the fastest episodes of subsidence prior to 30 Ma and again after 5.5 Ma, suggesting at least two stages of extension. The period 16–5.5 Ma is the slowest period and coincides with and postdates the folding and inversion seen in the seismic profiles (Figure 3), thus dividing the basin history into three distinct periods. It is noteworthy that the 5.5 Ma subsidence event is much more strongly developed in the southern basin and is not resolvable in the Hanoi basin or the Qiongdongnan basin away from the transition zone with the Yinggehai basin. These differences are possibly due to different responses to renewed tectonic stress in different parts of the basin [cf. *Burchfiel and Stewart*, 1966; *Crowell*, 1974]. *Rangin et al.* [1995] identified a strong erosion and inversion surface just predating the 5.5 Ma reflector in the Gulf of Tonkin region, not far from drill site K2-1X showing that active subsidence did affect this area in the Pliocene-Recent too.

7. Two-Dimensional Subsidence Analysis

[35] In rift basins the quantification of synrift and postrift subsidence can be used to quantify the degrees of crustal

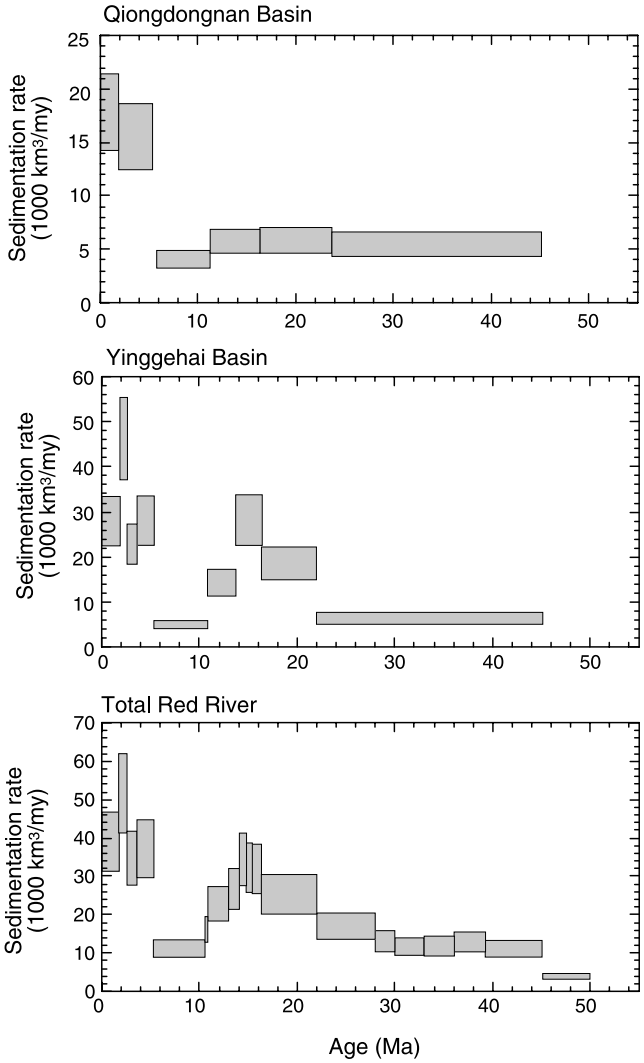

Figure 16. Reconstructed sediment budgets for (top) the Qiongdongnan basin, (middle) the southern Yinggehai basin covered by the data interpreted here, and (bottom) the entire Red River depositional system, including the onshore Hanoi basin, modified from budget of *Clift et al.* [2004].

and mantle extension [*McKenzie*, 1978; *Royden and Keen*, 1980], but in a pull-apart basin this is more complex because of the long duration of active basin formation (34–15 Ma in this case), and the difficulty of determining how long extension in a given location lasted. The crust and mantle extension are often decoupled in strike-slip environments, further complicating the subsidence analysis [*Roy and Royden*, 2000]. Nonetheless, a general impression of how crustal extension varies across the eastern margin of the Yinggehai basin can be derived from examining the sediment unloaded basement depths along one of the NE-SW oriented profiles from east of Hainan.

[36] The modern unloaded depth to basement along Profile 3599 is shown in Figure 18. If a uniform extension assumption is made then the total basement subsidence can be used to estimate total lithospheric extension using the instantaneous extension model of *McKenzie* [1978]. If we assume that the eastern strike slip basin margin was largely extended and formed as the basin began to subside after 34 Ma then we can estimate extension, as shown in Figure 18 (bottom). Although the oldest basin sediments date from the Eocene these are associated with modest regional extensional stress, similar to those seen in the Beibu and Pearl River Mouth basins [e.g., *Su et al.*, 1989; *Clift and Lin*, 2001], and are not linked to the main basin formation event as a pull-apart after 34 Ma. Not surprisingly β factor (defined as the preextensional crustal thickness divided by the postextensional) increases sharply from very low values close to Hainan, with large increases across the major bounding faults. Even if some of our assumptions are not valid the pattern (if not magnitudes) of crustal extension is not likely to be much different from that shown here. Because basement was not imaged at the southwestern end of the profile we can only constrain β to being at least 1.9 in that region. A simple backstripping analysis of an imaginary well in the 17 km deep basin center yields a maximum total β factor of 3.6, assuming a 34 Ma end to extension. If extension at 5.5 Ma was a significant part of the total extension then net β would be higher. A β of 3.6 is significant but is less than strongly thinned crust along a continent-ocean transition, indicating that despite great strike-slip motion the crust flooring the Yinggehai basin must still be continental.

8. Flexural Modeling Based on Measured Upper Crustal Extension

[37] A more detailed look at deformation mechanisms during basin formation can be achieved through a two-dimensional forward modeling method. This method can only be applied with confidence to the purely extensional Qiongdongnan basin, where the vast majority of the extension is oriented parallel to the section modelled. We do no attempt to apply this approach to the much more structurally complex Yinggehai basin. We have investigated the structure of the Qiongdongnan basin through modeling of Profiles C-37-79 and C-57-79 (Figure 2). We choose these profiles because basement is imaged across the entire profile of each section and because the faulting in each case is well defined from the seismic reflection data. The seismic data do not indicate that upper crustal strain was accommodated in any other fashion except through brittle faulting (i.e., not via magmatic extension).

[38] We employ the flexural cantilever model of *Kusznir et al.* [1991] to forward model the deformation and subsidence that would be expected to result from the extension measured across the normal faults identified on the seismic profiles (Figure 19). In this approach we make no attempt to replicate the basin morphology, but simply extend a model continental lithosphere using the faults seen on the seismic profiles and then predict what sort of basin this would form after 28 m.y. of postrift subsidence [*Clift et al.*, 2002b]. Although seafloor spreading initiated at ~30 Ma [*Briais et al.*, 1993], active extension in the Pearl River Mouth basin, east of Hainan, continued locally until 24 Ma, and at least until 28 Ma in most places [*Su et al.*, 1989; *Clift and Lin*, 2001]. Misfits between model and observation can thus be used to describe how the actual deformation in the ductile lower crust and mantle differed from the uniform pattern assumed by the model and calculated from the brittle

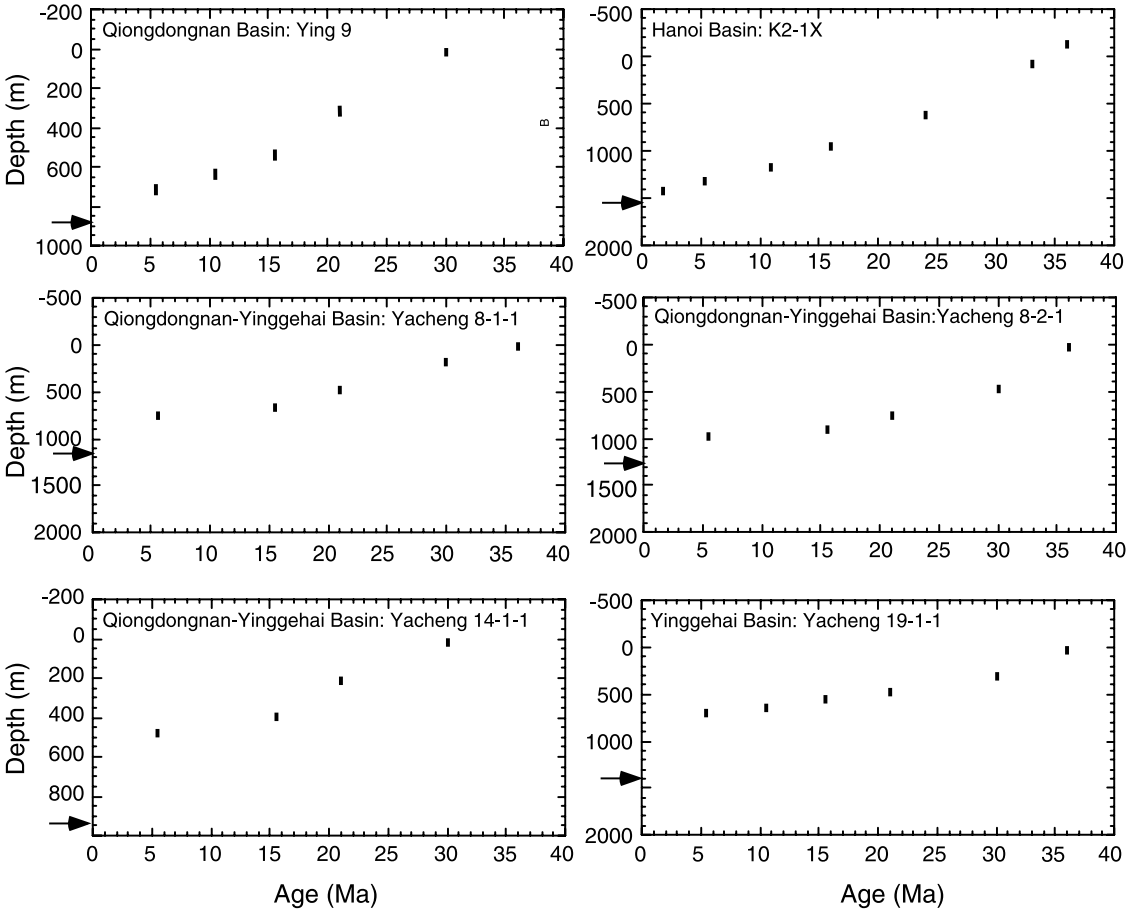

Figure 17. Results of one-dimensional backstripping analysis of well data from the Yinggehai–Song Hong region showing the sediment-unloaded depth to basement through Cenozoic time. Vertical solid bars indicate uncertainty in the water depths of deposition. Arrows at left-hand axes indicate modern unloaded depth to basement.

extension in the upper crust. The model assumes a Te of 3 km [*Bellingham and White*, 2000; *Clift et al.*, 2002b] and an initial crustal thickness of 35 km, sufficient to bring the unextended prerift crust to sea level.

8.1. Flexural Modeling Method

[39] The flexural cantilever model of *Kusznir and Egan* [1989] assumes the deformation of the plate being divided between a brittle upper crust, where simple shear along discrete faults is the prime mode of strain accommodation, and a ductile lower crust and mantle deforming in a sinusoid pure shear mode (Figure 19). Although a sinusoid is a simplification of the strain distribution, this assumption does mimic the expected strain distribution over long wavelengths in a plastic lower lithosphere. The flexural cantilever model defines the base of the lithosphere to be at the 1330°C isotherm, with a thickness of 125 km prior to extension. The model also assumes instantaneous extension. Application of this analytical method to rift systems, such as the North Sea [*Roberts et al.*, 1993] and East Africa [*Kusznir et al.*, 1995], as well as passive margin basins (e.g., Jeanne D'Arc basin [*Kusznir and Egan*, 1989]; Pearl River margin [*Davis and Kusznir*, 2004; *Clift et al.*, 2002b]) has achieved good matches of the rift architecture and sedimentary fill, allowing the lateral variability in extension to be modeled.

[40] Profile C-37-79 (Figure 20) shows an example of the method. In Figure 20 (top) we show the observed depth-converted profile, showing only the total sediment cover and the basement, while Figure 20 (bottom) shows the forward model based on the measured faulting. The most striking aspect is that the two are quite different from one another. The model does generate a number of deepwater basins, but across the entire model section the structural highs lie close to sea level and generally within the top 1 km. In contrast, in reality the structural highs at the southeastern end of Profile C-37-79 are 6–7 km subsea surface. This indicates that there is great deal more extension and subsidence in the margin than would be predicted from the brittle faulting alone and a uniform extension model.

[41] Assuming that the estimate of upper crustal faulting is accurate then the mismatch between observation and model can be used to quantify the distribution of strain along the Qiongdongnan margin. Although *Walsh et al.* [1991] suggested that as much as 40% of faulting might be too small to image from seismic profiles it seems unlikely that the seismic data would do a progressively worse job

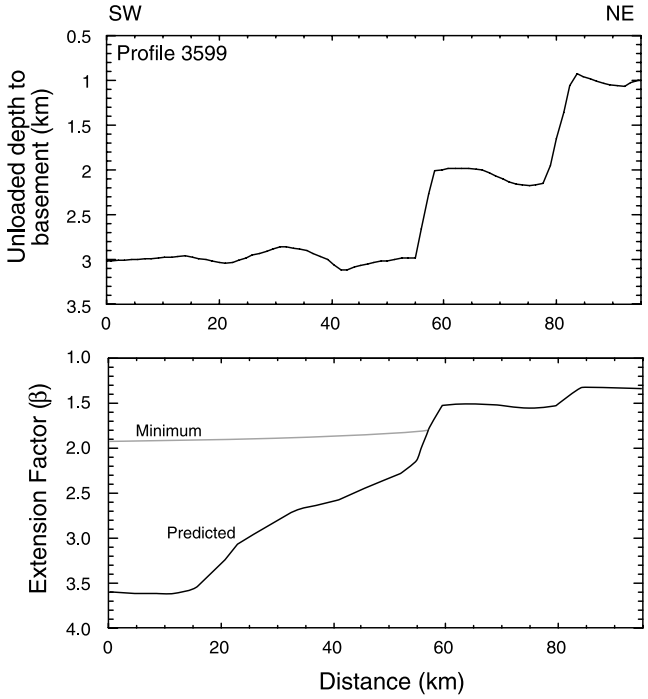

Figure 18. (top) Reconstruction of the unloaded depth basement along Profile 3599, perpendicular to the length of the Yinggehai basin. (bottom) Estimates of the total lithospheric extension (*b*) for the basin margin assuming instantaneous extension ending at 45 Ma. Dotted line shows the minimum β values based on the basement lying at the base of the seismic profile. Solid line shows prediction based on regional mapping of sediment thicknesses shown in Figure 11.

from one end of the section to another, since the mismatch is worse in deeper water. There is no suggestion that densification of the crust due to magmatic underplating has occurred, or that our estimates of extension are grossly in error because of an important component of magmatically accommodated extension. As a result the total accommodation space can be used to estimate the total crustal extension using the *McKenzie* [1978] uniform extension model. Consequently the lower crustal extension can be estimated by taking away the upper crustal extension (measured from the observed faulting) from the total crustal extension. In our study we calculate the lower crustal extension on the basis of brittle faulting terminating at 10 or 15 km depth. *Zuber et al.* [1986] assumed continental lithosphere with a quartz-dominated rheology and a geothermal gradient of 15–18°C/km to estimate the brittle ductile transition lying between 10 and 15 km depth, a range supported by the observed depth of seismic activity in most rifts [e.g., *Maggi et al.*, 2000].

8.2. Strain Distributions

[42] The distribution of strain across the Qiongdongnan margin is shown in Figure 21. Seafloor spreading did not reach this far west in the late Oligocene, but analysis of Profile C-57-79 shows that extension was great, with some crust approaching, or even exceeding the typical depth of 28 Ma oceanic crust [*Parsons and Sclater*, 1977]. Although the tilted fault block tectonic character and lack of marine magnetic anomalies [*Briais et al.*, 1993] clearly indicates that Profile C-57-79 only covers extended continental crust, and not oceanic crust, it is also plain that the degree of extension was so high as to be approaching the onset of seafloor spreading, except for at the northwest and southeast ends of the profile. In contrast, the extension at the northwest end of Profile C-37-79 is low, but increases rapidly to high values of β into deeper water. This means that Profile C-37-79 can better be used to understand the transition from the unrifted crust of Hainan Island into the South China sea, while Profile C-57-79 provides a detailed image of the highly extended crust in the basin center.

[43] It is apparent from the analysis of both profiles that the lower crust is always more extended than the upper crust, regardless of whether the brittle upper crustal faulting extended to 10 or 15 km depth. In practice this extra lower crustal extension is caused by the general underprediction of total subsidence by the forward models on the basis of upper crustal faulting alone. Profile C-37-79 shows that this difference between upper and lower crust extension becomes more extreme toward the southeast, as extension increases (Figure 21). Indeed, the northwesternmost 20 km of Profile C-37-79 shows almost identical degrees of upper and lower crustal (i.e., uniform) extension. The differences only become extreme oceanward of an inflexion point, which is defined on the basis of the

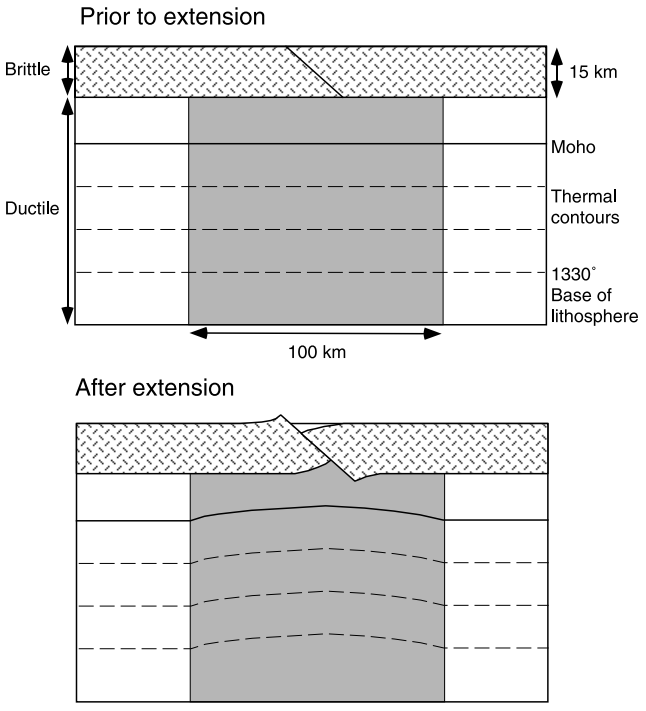

Figure 19. A schematic representation of the flexural cantilever model for lithospheric deformation showing assumptions of simple shear faulting in the brittle upper crust and the assumed same amount of pure shear in the lower crust and mantle (redrawn from *Kusznir et al.* [1991]). (Reproduced with permission from the Geological Society, London.)

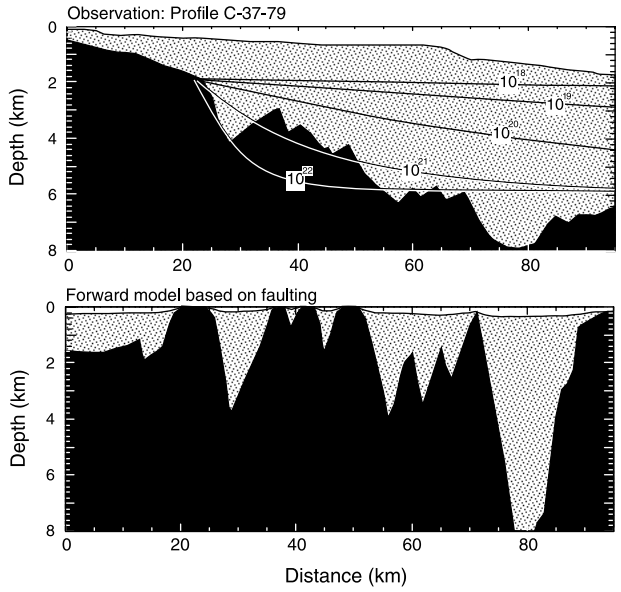

Figure 20. Comparison of observed depth-converted section across the Qiongdongnan basin (C-37-79) showing (top) the depth to basement and total sediment cover and (bottom) the basin geometry predicted using only the geometry and throw on the faults interpreted from the seismic data and the flexural cantilever model of *Kusznir et al.* [1991] shown in Figure 19. Although the model does predict some deep basins, the structural highs across the entire model profile come close to sea level, in sharp contrast to the increasing depth across the observed profile. Figure 20 (top) compares the modern profile with predicted profiles for crust assuming a viscous lower crustal channel 15 km thick and with variable viscosity, labeled in units of Pa s [modified from *Clark and Royden*, 2000].

strongly increasing lower crustal extension [*Clift et al.*, 2002b]. In this respect the Qiongdongnan margin closely resembles the great degrees of lower crustal extension predicted from the oceanward end of the Pearl River Mouth basin [*Clift et al.*, 2002b; *Davis and Kusznir*, 2004]. It is also noteworthy that despite its much thinner sedimentary cover the degrees of extension in the Qiongdongnan basin greatly exceed those in the central Yinggehai basin. The lack of correlation between the overlying sediment thickness and the degree of preferential lower crustal extension argues against the deformation here being a response to sediment loading, such as seen in the Pattani and Malay basins [cf. *Hall and Morley*, 2004]. The link with total crustal extension instead indicates that the preferential lower crustal loss is due to processes operational during the initial basin formation.

9. Discussion

[44] The reconstruction and quantification of the generation and filling of the Yinggehai–Song Hong and Qinongdongnan basins has important implications for several aspects of our understanding of the erosional and tectonic history of east Asia, and by extension on our overall comprehension of what processes control erosion and the interaction of the solid Earth and climate. We now discuss some of the more important issues raised by this work.

9.1. Sediment Budgets and Erosion

[45] The reconstructed sediment budgets for the Qiongdongnan and Yinggehai basins (Figure 16) are generally consistent with the model of a wedge of sediment delivered by the Red River progressively filling the Yinggehai basin from its northern end and only overspilling into the Qiongdongnan basin as tectonic subsidence in the Yinggehai basin slowed and the flux of sediment increased in the Pliocene. The increased Pliocene sedimentation in the Qiongdongnan basin is also consistent with tectonic and volcanic data that indicate strong activity in the region around Hainan since the Pliocene and especially since 2 Ma [*Tu et al.*, 1991; *Flower et al.*, 1998]. Although *Carter et al.* [2000] have reconstructed rapid cooling and erosion in the Central Highlands of Vietnam after ~8 Ma this region is not thought to be important as a source of sediment to the Yinggehai basin, but should be influential in the Mekong offshore region [*Clift et al.*, 2004]. 8 Ma is actually reconstructed as a time of reduced sediment flux to the Yinggehai basin. The rapid exhumation in the Central Highlands is spatially associated with synchronous magmatism that is limited to southern parts of Indochina, outside the Yinggehai–Song Hong catchment. There is no suggestion that this event affected the Vietnam coast south of the Red River delta. Moreover, the southward infilling history of the basin and the observation of south and west prograding clinoforms provides no clues to that part of Vietnam being important to the sediment budget.

[46] The budget we present here differs from that published by *Métivier et al.* [1999] in having a major middle Miocene peak, while that earlier reconstruction emphasized only the importance of the Pliocene-Recent as a time of fast erosion. It is noteworthy that the best hydrocarbon reservoirs in the Yinggehai basin are in middle Miocene sandstones, consistent with the idea of this being a time of increased coarse clastic flux. Falling sedimentation rates in the late Miocene also parallel the work of *Burbank et al.* [1993] on the Ganges-Brahmaputra system, albeit with less precise age control in the Yinggehai basin. The mismatch with the budget of *Métivier et al.* [1999] is noteworthy, however, and is explicable in terms of the data used. Unless data from shallow and deepwater regions of the margins are integrated then variations in sea level can result in biases in the reconstructed sediment budget that do not reflect changes in continental erosion rate. Because sea level fell from 14 to 10 Ma [*Haq et al.*, 1987] sedimentation would have fallen on the Yinggehai shelf even in the case of a constant sediment supply. However, by also documenting the deeper water part of the system in the Qiongdongnan region we are able to account for the changing location of the depocenter and derive a sediment budget that is independent of sea level.

[47] Enhanced sedimentation in the middle Miocene has been noted in several other east Asian basins [*Clift et al.*, 2004], in the Arabian Sea [*Clift and Gaedicke*, 2002], offshore West Africa [*Lavier et al.*, 2001], in the European Alpine foreland basins [*Kuhlemann et al.*, 2002] and on the eastern seaboard of North America [*Steckler et al.*, 1999]. Sedimentation in the Mediterranean Sea also appears to

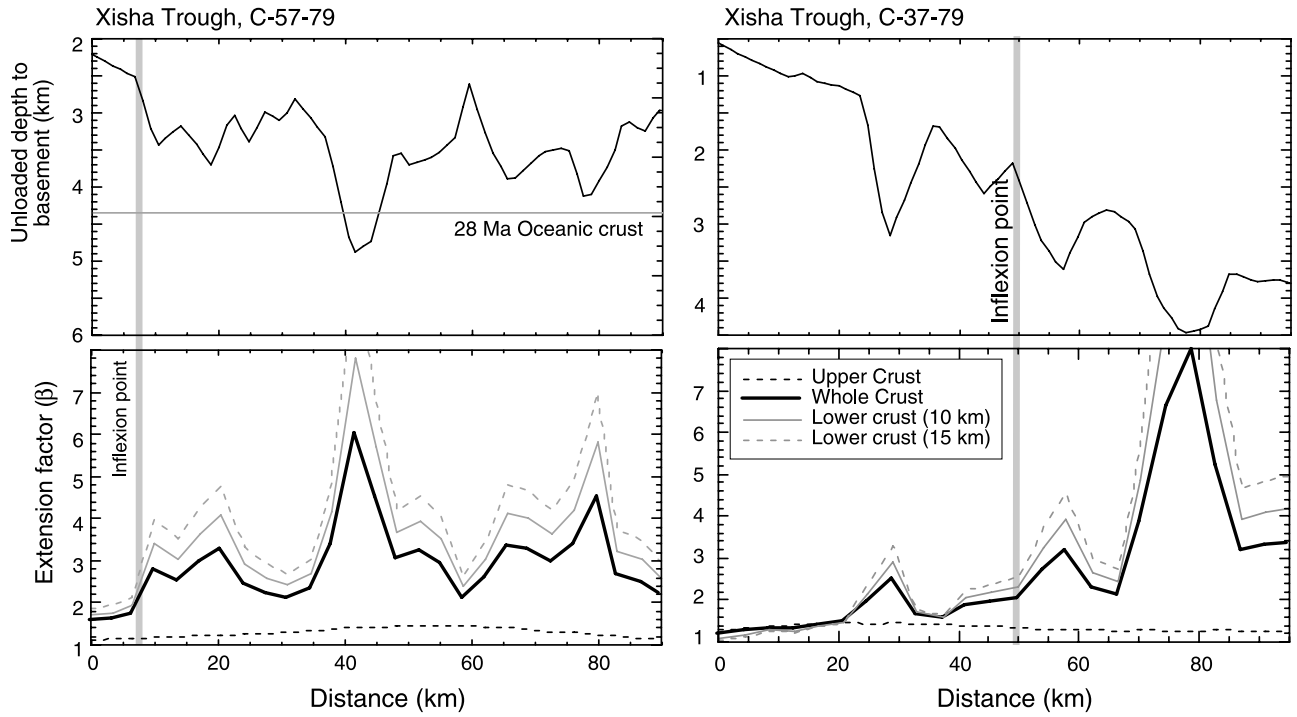

Figure 21. Calculated upper, whole, and lower crustal extension factors (*b*) across the Qiongdongnan across-margin Profiles C-37-79 and C-57-79. Lower crustal extension is shown assuming a depth of brittle faulting to both 10 km and 15 km. Note the general pattern of greater lower crustal extension compared to the upper crust, especially approaching deeper water in Profile C-37-79.

have become more clastic at the same time [*John et al.*, 2003]. Although some of these studies suggested that faster erosion was linked to tectonically driven uplift in the source region, the suggestion that enhanced erosion might be global lead *Steckler et al.* [1999] to propose a climatic mechanism for this erosional pulse. The lack of middle Miocene tectonism in eastern North America is strongly suggestive of a dominant climatic control at that time. What is clear is that climatic instability due to the 20 and 40 k.y. cycles of glacial-interglacial activity since ~3 Ma cannot be the only major influence on continental erosion [cf. *Zhang et al.*, 2001; *Molnar*, 2004].

[48] The faster erosion seen in the Red River system during the middle Miocene predates the onset of Northern Hemispheric glaciation and so requires that some other process must be driving this. Tectonically generated rock uplift in the source regions may be a crucial control on erosion [e.g., *Burbank et al.*, 2003]. It is noteworthy that rapid cooling of the metamorphic rocks that now form the Ailao Shan along the Red River fault zone began their exhumation after 34 Ma [*Gilley et al.*, 2003]. However, these rocks had slowed their ascent by around 25 Ma [*Harrison et al.*, 1996; *Wang et al.*, 1998; *Leloup et al.*, 2001], so that their exhumation cannot be the cause of the middle Miocene peak. Uplift of the eastern Tibetan Plateau is a controversial topic with almost as many suggested uplift ages as there are workers on the topic (see review in *Harris* [2006]). Although dating of extensional faulting on the plateau was initially used to constrain when the plateau reached maximum altitude [e.g., *Harrison et al.*, 1992], new methods based on stable isotopes in continental sediments [*Rowley et al.*, 2001] and improved paleobotanical techniques [*Spicer et al.*, 2003] now predict that at least southern and central Tibet were elevated close to their present altitude before 15 Ma. Surface uplift prior to that time might have been expected to have caused incision of gorges along the flanks of the plateau and should contribute to the erosional flux offshore.

[49] The role of climate in controlling erosion is not easy to assess in the middle Miocene because of the poor reconstruction of continental climate at that time, yet some information is available from ODP Site 1148 on the southern China margin. *Clift et al.* [2002a] used clay minerals from that site to indicate the onset of wet conditions prior to 15 Ma. Similarly *Jia et al.* [2003] analyzed carbon isotope data to propose a change in continental vegetation and earlier episodic strengthening of the monsoon, perhaps back to 20 Ma. Most recently *Clift* [2006] presented clastic mass accumulation rate and color data from ODP Site 1148 to show an initial phase of wetter conditions in southern China shortly after 25 Ma, with conditions becoming more arid after 14 Ma. If stronger summer monsoon rains did begin to affect the region as early as the late Oligocene then this may be important in driving the enhanced erosion we have reconstruct here. Studies of modern mountain ranges show a close relationship between erosion and rainfall [e.g., *Galy and France-Lanord*, 2001; *Dadson et al.*, 2003; *Wobus et al.*, 2003; *Reiners et al.*, 2003]. Conversely a drying of the global and regional climate during the late Miocene could explain the

reduced sedimentary flux at that time [*Derry and France-Lanord*, 1996; *Cerling et al.*, 1997; *Dettman et al.*, 2001; *Gupta et al.*, 2004].

[50] The importance of precipitation, rather than glaciation, in controlling erosion in the Red River basin, is also supported by the observation that our reconstructed average sediment delivery rate for the Pleistocene is only $63–42 \times 10^6$ t/yr, while *Milliman and Syvitski* [1992] estimated a recent rate of 133×10^6 t/yr prior to major human disruption of the drainage. This indicates that the Red River was carrying much more sediment to the Yinggehai basin during the Holocene than it can have done on average during the Pleistocene. A similar pattern was identified in the Holocene of the Ganges-Brahmaputra delta [*Goodbred and Kuehl*, 2000]. This is an important observation because it implies that the wetter, stronger summer monsoon conditions that prevailed during the deglaciation [e.g., *Prins and Postma*, 2000; *Wang et al.*, 2001; *Fleitmann et al.*, 2003] caused increased erosion and sediment transport. Conversely there must have been periods, presumably during glacial periods, when erosion and runoff were below average because of the drier conditions that prevailed.

[51] The fact that the Red River seems to have experienced rapid short-term variations in its clastic load means that the sediment transport process from source to offshore basin is not significantly buffered by storage or erosion from flood plains onshore [cf. *Métivier and Gaudemer*, 1999]. This makes geological sense in the Red River system, where the river runs for much of its course through bedrock gorges and only passes over a small flood plain in the Hanoi basin before reaching the ocean. Thus the potential sediment storage space on flood plains is somewhat less in the Red River than is typical for many systems, and contrasts with the long, flat flood plains of the Changjiang and Mekong.

9.2. Sediment Budgets and Drainage Capture

[52] Interpretation of the Yinggehai sediment budget is complicated by the drainage capture that is proposed to have influenced its headwaters during the uplift of the Tibetan Plateau [e.g., *Brookfield*, 1998; *Clark et al.*, 2004]. In these models the Red River was originally a much more extensive, dendritic drainage that originally included the headwaters of the modern Tsangpo, Salween, Mekong and Changjiang. These sections of river were progressively lost from the Red River as a result of compressive tectonism and elevation increase close to the eastern Himalayan syntaxis, especially in modern Yunnan. *Clift et al.* [2004] showed that there was more Miocene and Paleogene sediment in the Yinggehai basin that was eroded within the modern Red River drainage at those times, thus requiring the existence of a more widespread catchment in the past. Although capture events should result in reduced flow of sediment to the sea our sediment budgets cannot identify which drainage was lost at what time, which would require detailed budgets from the other river systems and provenance data from the sediments themselves.

[53] Despite these caveats the regional budget does allow some constraints to be placed on the timing of major drainage loss. The clastic flux has been high and shows no major falls since 5 Ma, indicating that any large capture must predate that time. The most striking fall in sediment rates occurs at 10.3–14 Ma, although because this is also a time of reduced sedimentation in the Indus, Irrawaddy, Gulf of Thailand and East China Sea [*Clift et al.*, 2004] it is not clear how much of this fall is driven by capture or by climate change. The fall in clastic accumulation rates in the Irrawaddy and East China Sea is especially noteworthy because these systems would be gaining drainage at the expense of the Red River if the capture model is correct. Nonetheless, it appears that the flux to the Yinggehai basin reached its lowest point around 10.3 Ma, which implies that major drainage loss had occurred before that time. Progressive capture could have occurred during the early Miocene-Oligocene if the loss of drainage was balanced by increased continental erosion yields caused by the strengthening of the summer monsoon precipitation.

[54] Assuming that models such as *Clark et al.* [2004] are correct to link drainage capture with regional surface uplift in eastern Tibet our data suggest that major regional surface uplift in eastern Tibet predated 10.3 Ma, consistent with the elevation reconstructions of *Rowley et al.* [2001] and *Spicer et al.* [2003], but in conflict with models that emphasize major uplift starting around 8 Ma [e.g., *Harrison et al.*, 1992; *Molnar et al.*, 1993; *Wang*, 2004]. In particular our data suggest that the 9–13 Ma gorge incision measured in Yunnan by *Clark et al.* [2005] must be a largely local phenomenon, and not representative of wide regions of eastern Tibet.

9.3. Tectonics of the Red River Fault Zone

[55] The Red River fault zone is one of the classic strike-slip faults of east Asia that in some tectonic models for strain accomodation are responsible for the large-scale displacement of Asian continental crustal blocks to the East because of the indentation of India with the active margin of Asia [e.g., *Molnar and Tapponnier*, 1975; *Armijo et al.*, 1989; *Tapponnier et al.*, 2001; *Replumaz and Tapponnier*, 2003]. Because the Yinggehai basin is formed largely by shearing along this zone our seismic stratigraphy allows some broad temporal constraints to be placed on the activity of the fault. Dating of the oldest sedimentary rocks in the Yinggehai basin indicate initial subsidence around 45 Ma, which is before the start of shearing on the Red River fault zone dated by *Gilley et al.* [2003]. In this scenario, the Eocene subsidence of the Yinggehai basin is likely linked to the earlier extension identified in the Beibu and Pearl River Mouth basins [*Su et al.*, 1989; *Clift and Lin*, 2001; *Zhou et al.*, 2002]. Well data show that basement subsidence in the Yinggehai basin was most rapid after around 34 Ma (Figure 17), coincident with the start of motion on the Red River fault zone and thus a dominant pull-apart origin, consistent with the basin's location geometry and tectonic architecture. The oldest sedimentary rocks found in wells considered in this study are dated at 36 Ma (uppermost Eocene), in the northern Qiongdongnan basin at Yacheng 8-2-1 and in the Hanoi basin at K2-1X (Figures 1 and 2). Both these wells penetrate to prerift basement but because they are positioned on the edge of the basin they likely do not preserve the oldest material.

[56] Thermochronology work by *Harrison et al.* [1996], *Wang et al.* [1998], *Leloup et al.* [2001] and *Gilley et al.* [2003] indicates faulting and exhumation starting around 34 Ma, consistent with the offshore stratigraphy. These studies

also suggest rapid left-lateral deformation until ~17 Ma, just after the first major inversion of the northern Yinggehai basin and just before that in the southern part of the basin, shown by folding and ponding of sediments on Profile 4540 (Figure 3) prior to 13.8 Ma. We interpret the inversion to be driven by a change in the stress field at that time. *Zhong et al.* [2004] suggested that the fault inversion and folding in the northwestern part of the basin occurred from late Oligocene to early Miocene because of the south-southeastward movement of the Indochina block along roughly NS-trending boundary faults, a process that those authors interpreted as driving the southward migration of the depocenter during the late Oligocene-early Miocene we observe here.

[57] Basement subsidence after inversion was slow. The youngest tectonic event in the Yinggehai basin is the apparent basement subsidence event at 5.5 Ma, which does not have an equivalent thermochronologic event in the Red River fault zone. However, if motion was limited and exhumation shallow onshore then this might not be recorded in standard thermochronometers that typically require at least 2 km of exhumation (60°C cooling) in order to be preserved. It is noteworthy that renewed subsidence after 5.5 Ma is accompanied by active faulting in the Yinggehai basin (Figures 4c and 5). Because of the low uncertainties in the water depth estimates there is little doubt that this event is a real basement tectonically driven subsidence event and does not reflect simple sediment loading. The origin of this event is not known, but could relate to the start of right-lateral deformation, which is believed to be influencing the modern Red River fault zone. The possible influence of the proposed Hainan Plume [*Tu et al.*, 1991; *Flower et al.*, 1998; *Lebedev and Nolet*, 2003] on the vertical tectonics of the Yinggehai basin is not known, although the basement subsidence reconstructions do not show resolvable uplift coincident with the volcanism in Hainan at this time.

9.4. Extensional Tectonics of the South China Sea

[58] Our reconstruction of the deformation of the Qiongdongnan basin adds to the debate concerning the nature of strain accommodation during continental breakup in the South China Sea. Our modeling of Profiles C-37-79 and C-57-79 (Figure 21) is consistent with similar work from the margin east of Hainan in showing preferential lower crustal extension approaching the continent-ocean transition [*Clift et al.*, 2002b; *Davis and Kusznir*, 2004]. Lower crustal extension accelerates seaward of an inflexion point, landward of which extension was much less and with generally comparable degrees of lower and upper crustal extension. The deformation appears to be a form of depth-dependent extension rather than being related to a detachment separating the upper and lower crust, because the highest degrees of lower crustal extension coincide with areas of increased extension in the upper crust [cf. *Driscoll and Karner*, 1998]. There is no evidence to suggest that increased lower crustal extension in the Qiongdongnan basin is mirrored by less extension on the southern edge of Xisha trough. It is noteworthy that in the case of the Qiongdongnan basin there was no seafloor spreading directly offshore and this implies loss of the lower crust not only oceanward but along the strike of the margin, presumably toward the propagating seafloor spreading center. The degree of extension is very high locally, allowing deep sag basins to develop. The degree of extension in the deep basin on Profile C-37-79 implies a postrift crustal thickness of <5 km under the subbasin center.

[59] The extension is so high in the center of the basin that we must consider the possibility that some of the extension was accommodated by magmatic crustal accretion, such as diking. If this were an important process then this could partially explain the subsidence deficit predicted only from extension on brittle faults. However, Profile C-37-79 shows a well defined, series of tilted fault blocks can be traced right across the section, with no suggestion of synrift volcanism. Seismic data from the Pearl River margin, further east do show clear volcanic edifices close to the continent-ocean transition, so there is no reason to believe that magmatic products are present but not imaged. As result we do not believe that magmatically accommodated extension was important in the formation of the Qiongdongnan basin. These data also help rule out the possible influence of magmatic driven densification of the crust as a mechanism for causing more subsidence than is predicted from the normal faulting in this area [cf. *Mahatsente et al.*, 1999].

[60] Preferential lost of the lower crust is interpreted to reflect ductile flow in this lithospheric level. Modeling by *Hopper and Buck* [1998] showed that lower crustal flow might be expected for a range of heat flow values when the continental crust is 30 km thick, and when quartz is the dominant mineralogy, as is likely here. Finite element theoretical models of passive margin formation (e.g., Baltimore Canyon trough [*Sawyer and Harry*, 1991]) have predicted an oceanward flow of lower crustal material from under opposing conjugate margins and the same process is invoked to explain the flat Moho under highly extended regions in the American Basin and Range Province [e.g., *Block and Royden*, 1990]. If such flow did occur in the Qiongdongnan basin then this material must be present oceanward of the extended upper crust and mantle, and implies a weak, low-viscosity lower crust. We conclude that this lower crustal flow occurred during active rifting. *Hall and Morley* [2004] have argued that loading by sediments has driven lower crustal flow in the Pattani and Malay basins, but this model is not appropriate here because the degree of "excess" extension increases as total extension increases, and shows no correlation with the total sediment thickness, which is greater closer to the coast of Hainan.

[61] We here compare our margin profiles with the model of *Clark and Royden* [2000] in which flow in the lower crust is modeled as a 15-km-thick channel. Although *Wernicke* [1990] suggested a range of 5–25 km for such lower crustal channels, 15 km is appropriate given estimates of the ductile layer under the South China Margin (10–15 km) and the total crustal thickness. Figure 20 shows the predicted profiles for a variety of crustal viscosities compared to the basement of Profile C-37-79. We place the theoretical curves from *Clark and Royden* [2000] against the observed basement, starting at the edge of the relatively unrifted edge of Hainan Island, so that we might determine the viscosity of the lower crust under the zone of lower crustal flow. The rifted basement is rougher than the model because of the formation of fault blocks. However, the

overall slope of the margin basement is most consistent with a model with lower crustal viscosity of 10^{21} Pa s. This number is comparable to the values derived by *Clift et al.* [2002b] for the Pearl River Mouth basin immediately east of Hainan and confirms that the lower crust around Hainan is more viscous than that further east, where lower crustal viscosity falls to 10^{19} Pa s. This viscosity difference is interpreted to reflect the greater extension in that region, where seafloor spreading has occurred and the existence of hotter, weaker crust linked to the presence of an earlier active margin offshore southeastern China. Despite this greater viscosity the Qiongdongnan basin appears to have suffered lower crustal flow over a zone at least 40–50 km wide.

10. Conclusions

[62] The Yinggehai–Song Hong basin is one of the largest strike-slip basins on Earth and is filled with as much as 17 km of sediment eroded largely from the eastern flanks of the Tibetan Plateau and delivered by the Red River. The basin started to open as a result of initial NNW-SSE extension after ~45 Ma, followed by dominant transtensional stresses starting around 34 Ma. These events are approximately synchronous with the extension observed from the northern margin of South China Sea. However, while extension in that margin was largely finished by 24–30 Ma, the Yinggehai basin continued to actively subside until it inverted in a diachronous fashion between 21 and ~14 Ma because of a change in the regional stress field. Extension resulted in a maximum β of around 3.6 in the central Yinggehai basin, where 17 km of sediments have accumulated. However, extension in the less sedimented Qiongdongnan basin was much higher, approaching β = 8 locally and with evidence for preferential thinning of the lower crust due to flow in a regime of depth-dependent stretching. The last active tectonic event was a subsidence event affecting the Yinggehai basin after 5.5 Ma.

[63] Sediments have filled the two basins from north to south with most sediment delivered from the Red River into the Yinggehai basin, where the depocenter has migrated south through time since the Oligocene. Sediment unloading and decompaction calculations allow a sedimentary budget to be determined for the region that is characterized by peaks in sediment delivery during the middle Miocene and during the Plio-Pleistocene. Sedimentation was most rapid during the late Pliocene (2.0–2.6 Ma) and is marked by development of large south-migrating foresets. At the same time shale diapirs were injected into the section, probably triggered by the rapid deposition of sediment and resultant increase in overpressuring. Seismic velocity analysis shows that overpressuring of the Miocene-Pliocene continues in the southern Yinggehai basin, although diapirism is not now active. Rapid sedimentation in the Plio-Pleistocene reflects fast erosion caused by the glacial-interglacial climate, though with most erosion occurring in the wetter interglacial periods. Tectonically driven uplift of Hainan, linked to magmatism during the Pleistocene [*Tu et al.*, 1991; *Flower et al.*, 1998], has also increased erosion from that source area.

[64] Fast sedimentation during the early-middle Miocene is believed to reflect a wetter, possibly monsoonal, climate at that time compared to the drier late Miocene and is inconsistent with monsoon strengthening at 8 Ma [cf. *Quade et al.*, 1989; *Kroon et al.*, 1991; *Prell et al.*, 1992]. Regional surface uplift in the eastern Tibetan Plateau likely also contributed to faster sedimentation during the early-middle Miocene, as a result of gorge incision. The sediment budget indicates that large-scale drainage capture away from the Red River system occurred before 10.3 Ma, although the falling erosion at 14–10.3 Ma parallels similar trends throughout Asia and does not necessarily reflect loss from the Red River at that time.

[65] **Acknowledgments.** The data used in this study were released by an agreement with the Chinese National Offshore Oil Company (CNOOC) and BP Exploration Operating Company Ltd. and through the help of the Vietnamese Petroleum Institute (VPI). We are grateful to Gerry Hey at BP Exploration and David Pullinger at Fugro-Robertsons for their generous help in providing data for this study. Lu Ming and CNOOC (Nanhai West) are thanked for providing additional data from the Yinggehai basin. Alan Roberts and Nick Kusznir are thanked for their donation of the Flex-Decomp™ and Stretch™ software packages. P.C. wishes to thank VPI and especially Nguyen Huy Quy and Nguyen Anh Duc for their help and advice in studying the Song Hong basin. Jason Ali, Xie Xinong, and Lu Ming are also thanked for their help with data and discussion of ideas. This work was supported in part by the College of Physical Sciences, University of Aberdeen, and by the Royal Society of London. The work was completed during the tenure of a visiting fellowship at Universität Bremen from the Alexander von Humboldt Foundation. We thank Chris Morley, Tung-Yi (Tony) Lee, and Peter Cawood for their review comments which greatly improved the paper. This paper represents a contribution to IGCP 476 "Monsoons and Tectonics."

References

An, Z., J. E. Kutzbach, W. L. Prell, and S. C. Porter (2001), Evolution of Asian monsoons and phased uplift of the Himalaya-Tibetan plateau since late Miocene times, *Nature*, *411*, 62–66.

Armijo, R., P. Tapponnier, and H. Tonglin (1989), Late Cenozoic right-lateral strike-slip faulting in southern Tibet, *J. Geophys. Res.*, *94*, 2787–2838.

Bellingham, P., and N. J. White (2000), A general inverse method for modelling extensional sedimentary basins, *Basin Res.*, *12*, 219–226.

Berggren, W. A., D. V. Kent, C. C. Swisher, and M. P. Aubry (1995), Revised Cenozoic geochronology and chronostratigraphy, in *Geochronology, Time Scales and Global Stratigraphic Correlation*, edited by W. A. Berggren et al., *Spec. Publ. Soc. Econ. Paleontol. Mineral.*, *54*, 129–212.

Block, L., and L. H. Royden (1990), Core complex geometries and regional scale flow in the lower crust, *Tectonics*, *9*, 557–567.

Braitenberg, C., E. Pagot, Y. Wang, and J. Fang (2002), Bathymetry and crustal thickness variations from gravity inversion and flexural isostasy, in *Satellite Altimetry for Geodesy, Geophysics and Oceanography*, *Int. Assoc. Geodesy Symp.*, vol. 126, edited by C. Hwang, C. K. Shum, and J. Li, pp. 143–149, Int. Assoc. of Geodesy, Copenhagen, Denmark.

Briais, A., P. Patriat, and P. Tapponnier (1993), Updated interpretation of magnetic anomalies and seafloor spreading in the South China Sea: Implications for the tertiary tectonics of Southeast Asia, *J. Geophys. Res.*, *98*, 6299–6328.

British Oceanographic Data Centre (2003), *GEBCO Digital Atlas*, *Centenary Edition* [CD-ROM], Br. Oceanogr. Data Cent., Liverpool, U.K.

Brookfield, M. E. (1998), The evolution of the great river systems of southern Asia during the Cenozoic India-Asia collision: Rivers draining southwards, *Geomorphology*, *22*, 285–312.

Burbank, D. W., L. A. Derry, and C. France-Lanord (1993), Reduced Himalayan sediment production 8 Myr ago despite an intensified monsoon, *Nature*, *364*, 48–50.

Burbank, D. W., A. E. Blythe, J. Putkonen, B. Pratt-Sitaula, E. Gabet, M. Oskins, A. Barros, and T. P. Ojha (2003), Decoupling of erosion and precipitation in the Himalayas, *Nature*, *426*, 652–655.

Burchfiel, B. C., and J. H. Stewart (1966), "Pull-apart" origin of the central segment of Death Valley, California, *Bull. Geol. Soc. Am.*, *77*, 439–442.

Burchfiel, B. C., L. H. Royden, E. Wang, R. King, Z. Chen, Y. Liu, Z. Zhang, and Z. Zhao (1997), Cenozoic tectonic evolution around the eastern Himalayan syntaxis, *Eos Trans. AGU*, *78*(46), Fall Meet. Suppl., F173.

Burrus, J. (1998), Overpressure models for clastic rocks, their relation to hydrocarbon expulsion: A critical reevaluation, in *Abnormal Pressures in*

Hydrocarbon Environments, edited by B. E. Law, G. F. Ulmishek, and V. I. Slavin, *AAPG Mem.*, *70*, 35–63.

Carbotte, S. M., et al. (2004), New integrated data management system for Ridge000 and MARGINS research, *Eos Trans. AGU*, *85*(51), 553, 559.

Carter, A., D. Roques, and C. S. Bristow (2000), Denudation history of onshore central Vietnam: Constraints on the Cenozoic evolution of the western margin of the South China Sea, *Tectonophysics*, *322*, 265–277.

Cerling, T. E., J. M. Harris, B. J. MacFadden, M. G. Leakey, J. Quade, V. Elsenmann, and J. R. Ehleringer (1997), Global vegetation change through the Miocene/Pliocene boundary, *Nature*, *389*, 153–158.

Clark, M. K., and L. H. Royden (2000), Topographic ooze: Building the eastern margin of Tibet by lower crustal flow, *Geology*, *28*, 703–706.

Clark, M. K., L. M. Schoenbohm, L. H. Royden, K. X. Whipple, B. C. Burchfiel, X. Zhang, W. Tang, E. Wang, and L. Chen (2004), Surface uplift, tectonics, and erosion of Eastern Tibet from large-scale drainage patterns, *Tectonics*, *23*, TC1006, doi:10.1029/2002TC001402.

Clark, M. K., M. A. House, L. H. Royden, K. X. Whipple, B. C. Burchfiel, X. Zhang, and W. Tang (2005), Late Cenozoic uplift of southeastern Tibet, *Geology*, *33*, 525–528.

Clift, P. D. (2006), Controls on the erosion of Cenozoic Asia and the flux of clastic sediment to the ocean, *Earth Planet. Sci. Lett.*, *241*, 571–580.

Clift, P. D., and C. Gaedicke (2002), Accelerated mass flux to the Arabian Sea during the middle-late Miocene, *Geology*, *30*, 207–210.

Clift, P. D., and J. Lin (2001), Preferential mantle lithospheric extension under the South China margin, *Mar. Pet. Geol.*, *18*, 929–945.

Clift, P. D., J. I. Lee, M. K. Clark, and J. Blusztajn (2002a), Erosional response of South China to arc rifting and monsoonal strengthening recorded in the South China Sea, *Mar. Geol.*, *184*, 207–226.

Clift, P. D., J. Lin, and U. Barckhausen (2002b), Evidence of low flexural rigidity and low viscosity lower continental crust in the South China Sea, *Mar. Pet. Geol.*, *19*, 951–970.

Clift, P. D., G. D. Layne, and J. Blusztajn (2004), The erosional record of Tibetan uplift in the east Asian marginal seas, in *Continent-Ocean Interactions in the East Asian Marginal Seas*, *Geophys. Monogr. Ser.*, vol. 149, edited by P. D. Clift et al., pp. 255–282, AGU, Washington, D. C.

Crowell, J. C. (1974), Origin of late Cenozoic basins in southern California, in *Tectonics and Sedimentation*, edited by W. R. Dickinson, *Spec. Publ. Soc. Econ. Paleontol. Mineral.*, *22*, 190–204.

Cung, T. C., S. Dorobek, C. Richter, M. Flower, E. Kikawa, Y. T. Nguyen, and R. McCabe (1998), Paleomagnetism of late Neogene basalts in Vietnam and Thailand: Implications for the post-Miocene tectonic history of Indochina, in *Mantle Dynamics and Plate Interactions in East Asia*, *Geodyn. Ser.*, vol. 27, edited by M. F. J. Flower et al., pp. 289–299, AGU, Washington, D. C.

Dadson, S., et al. (2003), Links between erosion, runoff variability and seismicity in the Taiwan orogen, *Nature*, *426*, 648–651.

Davis, M., and N. Kusznir (2004), Depth-dependent lithospheric stretching at rifted continental margin, in *Rheology and Deformation of the Lithosphere at Continental Margins*, edited by G. D. Karner et al., pp. 92–137, Columbia Univ. Press, New York.

Derry, L. A., and C. France-Lanord (1996), Neogene Himalayan weathering history and river $^{87}Sr/^{86}Sr$: Impact on the marine Sr record, *Earth Planet. Sci. Lett.*, *142*, 59–74.

Dettman, D. L., M. J. Kohn, J. Quade, F. J. Ryerson, T. P. Ojha, and S. Hamidullah (2001), Seasonal stable isotope evidence for a strong Asian monsoon throughout the past 10.7 m.y., *Geology*, *29*, 31–34.

Driscoll, N. W., and G. D. Karner (1998), Lower crustal extension across the Northern Carnarvon basin, Australia: Evidence for an eastward dipping detachment, *J. Geophys. Res.*, *103*, 4975–4991.

Fang, H., S. Li, Z. Gong, and J. Yang (2000), Thermal regime, interreservoir compositional heterogeneities, and reservoir-filling history of the Dongfang gas field, Yinggehai basin, South China Sea: Evidence for episodic fluid injections in overpressured basins?, *AAPG Bull.*, *84*, 607–626.

Fleitmann, D., S. J. Burns, M. Mudelsee, U. Neff, J. Kramers, A. Mangini, and A. Matter (2003), Holocene forcing of the Indian monsoon recorded in a stalagmite from southern Oman, *Science*, *300*, 1737–1739.

Flower, M., K. Tamaki, and N. Hoang (1998), Mantle extrusion: A model for dispersed volcanism and DUPAL-like asthenosphere in east Asia and the western Pacific, in *Mantle Dynamics and Plate Interactions in East Asia*, *Geodyn. Ser.*, vol. 27, edited by M. F. J. Flower et al., pp. 67–88, AGU, Washington, D. C.

Galy, A., and C. France-Lanord (2001), Higher erosion rates in the Himalaya: Geochemical constraints on riverine fluxes, *Geology*, *29*, 23–26.

Gilley, L. D., T. M. Harrison, P. H. Leloup, F. J. Ryerson, O. M. Lovera, and J. H. Wang (2003), Direct dating of left-lateral deformation along the Red River shear zone, China and Vietnam, *J. Geophys. Res.*, *108*(B2), 2127, doi:10.1029/2001JB001726.

Gong, Z., and S. Li (1997), *Basin Analysis and Accumulation of Oil and Gas in the Northern Margin of the South China Sea*, Science Press, Beijing, 510 pp. (in Chinese).

Gong, Z., and S. Li (2004), *Dynamic research of oil and gas accumulation in northern marginal basins of South China Sea* (in Chinese), 339 pp., Science Press, Beijing.

Goodbred, S. L., and S. A. Kuehl (2000), Enormous Ganges-Brahmaputra sediment discharge during strengthened early Holocene monsoon, *Geology*, *28*, 1083–1086.

Guo, L., Z. Zhong, and L. Wang (2001), Regional tectonic evolution around Yinggehai basin of South China Sea, *Geol. J. China Univ.*, *7*, 1–12.

Gupta, A. K., R. K. Singh, S. Joseph, and E. Thomas (2004), Indian ocean high-productivity event (10–8 Ma): Linked to global cooling or to the initiation of the Indian monsoons?, *Geology*, *32*, 753–756.

Hall, R. (2002), Cenozoic geological and plate tectonic evolution of SE Asia and the SW Pacific: Computer-based reconstructions and animations, *J. Asian Earth Sci.*, *20*, 353–434.

Hall, R., and C. Morley (2004), Sundaland basins, in *Continent-Ocean Interactions in the East Asian Marginal Seas*, *Geophys. Monogr. Ser.*, vol. 149, edited by P. D. Clift et al., pp. 55–87, AGU, Washington, D. C.

Hamilton, W. (1979), Tectonics of the Indonesian region, *Geol. Surv. Pap. 1087*, pp. 0–345, U.S. Gov. Print. Off., Washington, D. C.

Hao, F., F. Sun, S. Li, and Q. Zhang (1995), Overpressure retardation of the organic matter maturation and petroleum generation: A case study from the Yinggehai and Qiongdongnan basins, South China Sea, *AAPG Bull.*, *79*, 551–562.

Hao, F., S. Li, Z. Gong, and J. Yang (2000), Thermal regime, interreservoir compositional heterogeneities, and reservoir-filling history of the Dongfang gas field, Yinggehai basin, South China Sea: Evidence for episodic fluid injections in overpressured basins?, *AAPG Bull.*, *84*, 607–626.

Haq, B. U., J. Hardenbol, and P. R. Vail (1987), Chronology of fluctuating sea levels since the Triassic, *Science*, *235*, 1156–1167.

Harris, N. B. W. (2006), The elevation of the Tibetan Plateau and its impact on the monsoon, *Palaeogeogr. Palaeoclimatol. Palaeoecol*, in press.

Harrison, T. M., P. Copeland, W. S. F. Kidd, and A. Yin (1992), Raising Tibet, *Science*, *255*, 1663–1670.

Harrison, T. M., P. H. Leloup, F. J. Ryerson, P. Tapponnier, R. Lacassin, and W. Chen (1996), Diachronous initiation of transtension along the Ailao Shan-Red River shear zone, Yunnan and Vietnam, in *The Tectonic Evolution of Asia*, edited by A. Yin and T. M. Harrison, pp. 208–226, Cambridge Univ. Press, New York.

He, L., L. Xiong, and J. Wang (2002), Heat flow and thermal modeling of the Yinggehai basin, South China Sea, *Tectonophysics*, *351*, 245–253.

Holloway, N. H. (1982), North Palawan Block, Philippines—Its relation to Asian mainland and role in evolution of South China Sea, *AAPG Bull.*, *66*, 1355–1383.

Hopper, J. R., and W. R. Buck (1998), Styles of extensional decoupling, *Geology*, *26*, 699–702.

Jahn, B., P. Y. Chen, and T. P. Yen (1976), Rb-Sr ages of granitic rocks from southeastern China and their tectonic significance, *Bull. Geol. Soc. Am.*, *87*, 763–776.

Jia, G., P. Peng, Q. Zhao, and Z. Jian (2003), Changes in terrestrial ecosystem since 30 Ma in east Asia: Stable isotope evidence from black carbon in the South China Sea, *Geology*, *31*, 1093–1096.

John, C. M., M. Mutti, and T. Adatte (2003), Mixed carbonate-siliciclastic record on the North African margin (Malta): Coupling of weathering processes and mid Miocene climate, *Geol. Soc. Am. Bull.*, *115*, 217–229.

Kroon, D., T. Steens, and S. R. Troelstra (1991), Onset of monsoonal related upwelling in the western Arabian Sea as revealed by planktonic foraminifers, *Proc. Ocean Drill. Program Sci. Results*, *117*, 257–263.

Kuhlemann, J., W. Frisch, B. Székely, I. Dunkl, and M. Kázmér (2002), Post-collisional sediment budget history of the Alps: Tectonic versus climatic control, *Int. J. Earth Sci.*, *91*, 818-37.

Kusznir, N. J., and S. S. Egan (1989), Simple-shear and pure-shear models of extensional sedimentary basin formation: Application to the Jean d'Arc basin, Grand Banks of Newfoundland, in *Extensional Tectonics and Stratigraphy of the North Atlantic Margins*, edited by A. J. Tankard and H. R. Balkwill, *AAPG Mem.*, *46*, 305–322.

Kusznir, N. J., G. Marsden, and S. S. Egan (1991), A flexural cantilever simple shear/pure shear model of continental extension, in *The Geometry of Normal Faults*, edited by A. M. Roberts et al., *Geol. Soc. Spec. Publ.*, *56*, 41–61.

Kusznir, N. J., A. M. Roberts, and C. K. Morley (1995), Forward and reverse modelling of rift basin formation, in *Hydrocarbon Habitat in Rift Basins*, edited by J. J. Lambiase, *Geol. Soc. Spec. Publ.*, *80*, 33–56.

Lacassin, R., H. Maluski, P. H. Leloup, P. Tapponnier, C. Hinthing, K. Siribhakdi, S. Chuaviroj, and A. Charoenravat (1997), Tertiary diachronic extrusion and deformation of western Indochina: Structural and $^{40}Ar/^{39}Ar$ evidence from NW Thailand, *J. Geophys. Res.*, *102*, 10,013–10,037.

Lavier, L. L., M. S. Steckler, and F. Brigaud (2001), Climatic and tectonic controls on the Cenozoic evolution of the West African margin, *Mar. Geol.*, *178*, 63–80.

Lebedev, S., and G. Nolet (2003), Upper mantle beneath Southeast Asia from S velocity tomography, *J. Geophys. Res.*, *108*(B1), 2048, doi:10.1029/2000JB000073.

Leloup, P. H., T. M. Harrison, F. J. Ryerson, W. Chen, Q. Li, P. Tapponnier, and R. Lacassin (1993), Structural, petrological and thermal evolution of a Tertiary ductile strike-slip shear zone, Diancang Shan, Yunnan, *J. Geophys. Res.*, *98*, 6715–6743.

Leloup, P. H., N. Arnaud, R. Lacassin, J. R. Kienast, T. M. Harrison, P. Trinh, A. Replumaz, and P. Tapponnier (2001), New constraints on the structure, thermochronology, and timing of the Ailao Shan-Red River shear zone, SE Asia, *J. Geophys. Res.*, *106*, 6683–6732.

Lepvrier, C., H. Maluski, V. T. Vu, A. Leyreloup, T. T. Phan, and V. V. Nguyen (2004), The Early Triassic Indosinian orogeny in Vietnam (Truong Son Belt and Kontum Massif): Implications for the geodynamic evolution of Indochina, *Tectonophysics*, *393*, 87–118.

Liu, Z., Q. Wang, H. Yuan, and D. Su (1985), The Bouger anomalies and depths of Mohorovicic discontinuity in the South China Sea region, *Acta Oceanogr. Sin.*, *4*, 579–590.

Lu, W., C. Ke, J. Wu, J. Liu, and C. Lin (1987), Characteristics of magnetic lineations and tectonic evolution of the South China Sea basin, *Acta Oceanogr. Sin.*, *6*, 577–588.

Maggi, A., J. A. Jackson, D. P. McKenzie, and K. Priestley (2000), Earthquake focal depths, effective elastic thickness, and the strength of the continental lithosphere, *Geology*, *28*, 495–498.

Mahatsente, R., G. Jentzsch, and T. Jahr (1999), Crustal structure of the main Ethiopian rift gravity data: 3-dimensional modeling, *Tectonophysics*, *313*, 363–382.

McKenzie, D. P. (1978), Some remarks on the development of sedimentary basins, *Earth Planet. Sci. Lett.*, *40*, 25–32.

Metcalfe, I. (1996), Pre-Cretaceous evolution of SE Asian terranes, in *Tectonic Evolution of Southeast Asia*, edited by R. Hall and D. Blundell, *Geol. Soc. Spec. Publ.*, *106*, 97–122.

Métivier, F., and Y. Gaudemer (1999), Stability of output fluxes of large rivers in south and east Asia during the last 2 million years: Implications on floodplain processes, *Basin Res.*, *11*, 293–303.

Métivier, F., Y. Gaudemer, P. Tapponnier, and M. Klein (1999), Mass accumulation rates in Asia during the Cenozoic, *Geophys. J. Int.*, *137*, 280–318.

Miller, K. G., R. G. Fairbanks, and G. S. Mountain (1987), Tertiary oxygen isotope synthesis, sea level history, and continental margin erosion, *Paleoceanography*, *2*, 1–19.

Milliman, J. D., and J. P. M. Syvitski (1992), Geomorphic/tectonic control of sediment discharge to the ocean: The importance of small mountainous rivers, *J. Geol.*, *100*, 525–544.

Molnar, P. (2004), Late Cenozoic increase in accumulation rates of terrestrial sediment: How might climate change have affected erosion rates, *Ann. Rev. Earth Planet. Sci.*, *32*, 67–89.

Molnar, P., and P. Tapponnier (1975), Cenozoic tectonics of Asia: Effects of a continental collision, *Science*, *189*, 419–426.

Molnar, P., P. C. England, and J. Martinod (1993), Mantle dynamics, the uplift of the Tibetan Plateau, and the Indian monsoon, *Rev. Geophys.*, *31*, 357–396.

Morley, C. K. (2002), A tectonic model for the Tertiary evolution of strike-slip faults and rift basins in SE Asia, *Tectonophysics*, *347*, 189–215.

Packham, G. (1996), Cenozoic SE Asia: Reconstructing its aggregation and reorganization, in *Tectonic Evolution of Southeast Asia*, edited by R. Hall and D. Blundell, *Geol. Soc. Spec. Publ.*, *106*, 123–152.

Parsons, B., and J. G. Sclater (1977), An analysis of the variation of ocean floor bathymetry and heat flow with age, *J. Geophys. Res.*, *82*, 803–827.

Peltzer, G., and P. Tapponnier (1988), Formation and evolution of strike-slip faults, rifts, and basins during the India-Asia collision: An experimental approach, *J. Geophys. Res.*, *93*, 15,085–15,117.

Prell, W. L., and J. E. Kutzbach (1992), Sensitivity of the Indian monsoon to forcing parameters and implications for its evolution, *Nature*, *360*, 647–651.

Prell, W. L., D. W. Murray, S. C. Clemens, and D. M. Anderson (1992), Evolution and variability of the Indian Ocean summer monsoon: Evidence from the western Arabian Sea drilling program, in *Synthesis of Results From Scientific Drilling in the Indian Ocean*, *Geophys. Monogr. Ser.*, vol. 70, edited by R. A. Duncan et al., pp. 447–469, AGU, Washington, D. C.

Prins, M. A., and G. Postma (2000), Effects of climate, sea level, and tectonics unraveled for last deglaciation turbidite records of the Arabian Sea, *Geology*, *28*, 375–378.

Quade, J., T. E. Cerling, and J. R. Browman (1989), Dramatic ecologic shift in the late Miocene of northern Pakistan, and its significance to the development of the Asian monsoon, *Nature*, *342*, 163–166.

Rangin, C., M. Klein, D. Roques, X. Le Pichon, and L. V. Trong (1995), The Red River fault system in the Tonkin Gulf, Vietnam, *Tectonophysics*, *243*, 209–222.

Reiners, P. W., T. A. Ehlers, S. G. Mitchell, and D. R. Montgomery (2003), Coupled spatial variations in precipitation and long-term erosion rates across the Washington Cascades, *Nature*, *426*, 645–647.

Replumaz, A., and P. Tapponnier (2003), Reconstruction of the deformed collision zone between India and Asia by backward motion of lithospheric blocks, *J. Geophys. Res.*, *108*(B6), 2285, doi:10.1029/2001JB000661.

Roberts, A. M., G. Yielding, N. J. Kusznir, I. Walker, and D. Dorn-Lopez (1993), Mesozoic extension in the North Sea: Constraints from flexural backstripping, forward modelling and fault populations, in *Petroleum Geology of NW Europe: Proceedings of the* 4th *Conference*, edited by J. R. Parker, pp. 1123–1136, Geol. Soc. of London, London.

Rowley, D. B., R. T. Pierrehumbert, and B. S. Currie (2001), A new approach to stable isotope-based paleoaltimetry: Implications for paleoaltimetry and paleohypsometry of the High Himalaya since the late Miocene, *Earth Planet. Sci. Lett.*, *188*, 253–268.

Roy, M., and L. H. Royden (2000), Crustal rheology and faulting at strike-slip plate boundaries 2: Effects of lower crustal flow, *J. Geophys. Res.*, *105*, 5599–5613.

Royden, L., and C. E. Keen (1980), Rifting processes and thermal evolution of the continental margin of eastern Canada determined from subsidence curves, *Earth Planet. Sci. Lett.*, *51*, 714–717.

Ru, K., D. Zhou, and H. Chen (1994), Basin evolution and hydrocarbon potential of the northern South China Sea, in *Oceanology of China Seas*, vol. 2, edited by D. Zhou, Y. Liang, and C. Zeng, pp. 361–372, Springer, New York.

Sawyer, D. S., and D. L. Harry (1991), Dynamic modeling of divergent margin formation: Application to the U.S. Atlantic margin, *Mar. Geol.*, *102*, 29–42.

Schlüter, H. U., K. Hinz, and M. Block (1996), Tectono-stratigraphic terranes and detachment faulting of the South China Sea and Sulu Sea, *Mar. Geol.*, *130*, 39–78.

Sclater, J. G., and P. A. F. Christie (1980), Continental stretching: An explanation of the post mid-Cretaceous subsidence of the central North Sea basin, *J. Geophys. Res.*, *85*, 3711–3739.

Sewell, R. J., and S. D. G. Campbell (1997), Geochemistry of coeval Mesozoic plutonic and volcanic suites in Hong Kong, *J. Geol. Soc. Lond.*, *154*, 1053–1066.

Spicer, R. A., N. B. W. Harris, M. Widdowson, A. B. Herman, S. Guo, P. J. Valdes, J. A. Wolfe, and S. P. Kelley (2003), Constant elevation of southern Tibet over the past 15 million years, *Nature*, *421*, 622–624.

Steckler, M. S., G. S. Mountain, K. G. Miller, and N. Christie-Blick (1999), Reconstruction of Tertiary progadation and clinoform development on the New Jersey passive margin by 2-D backstripping, *Mar. Geol.*, *154*, 399–420.

Su, D., N. White, and D. McKenzie (1989), Extension and subsidence of the Pearl River mouth basin, northern South China Sea, *Basin Res.*, *2*, 205–222.

Sun, Z., D. Zhou, Z. Zhong, Z. Zeng, and S. Wu (2003), Experimental evidence for the dynamics of the formation of the Yinggehai basin, NW South China Sea, *Tectonophysics*, *372*, 41–58.

Sun, Z., Z. Zhong, D. Zhou, and Z. Zeng (2004), Continent-ocean interactions along the Red River fault zone, South China Sea, in *Continent-Ocean Interactions in the East Asian Marginal Seas*, *Geophys. Monogr. Ser.*, vol. 149, edited by P. D. Clift et al., pp. 109–120, AGU, Washington, D. C.

Tapponnier, P., G. Peltzer, and R. Armijo (1986), On the mechanics of the collision between India and Asia, in *Collision Tectonics*, edited by M. P. Coward and A. C. Ries, *Geol. Soc. Spec. Publ.*, *19*, 115–157.

Tapponnier, P., Z. Xu, F. Roger, B. Meyer, N. Arnaud, G. Wittlinger, and J. Yang (2001), Oblique stepwise rise and growth of the Tibet Plateau, *Science*, *294*, 1671–1677.

Taylor, B., and D. E. Hayes (1980), The tectonic evolution of the south China basin, in *The Tectonic and Geologic Evolution of Southeast Asian Seas and Islands*, *Geophys. Monogr. Ser.*, vol. 23, edited by D. E. Hayes, pp. 89–104, AGU, Washington, D. C.

Taylor, B., and D. E. Hayes (1983), Origin and history of the South China Sea basin, in *The Tectonic and Geologic Evolution of Southeast Asian Seas and Islands: Part 2*, *Geophys. Monogr. Ser.*, vol. 27, edited by D. E. Hayes, pp. 23–56, AGU, Washington, D. C.

Tu, K., M. F. J. Flower, R. W. Carlson, M. Zhang, and G. Xie (1991), Sr, Nd, and Pb isotopic compositions of Hainan basalts (south China): Implications for a subcontinental lithosphere Dupal source, *Geology*, *19*, 567–569.

Walsh, J., J. Watterson, and G. Yielding (1991), The importance of small-scale faulting in regional extension, *Nature*, *351*, 391–393.

Wang, P. (2004), Cenozoic deformation of Asia and the history of sea-land interactions in Asia, in *Continent-Ocean Interactions in the East Asian Marginal Seas*, *Geophys. Monogr. Ser.*, vol. 149, edited by P. D. Clift et al., pp. 1–23, AGU, Washington, D. C.

Wang, P. L., C. H. Lo, T. Y. Lee, S. L. Chung, C. Y. Lan, and N. Trong Yem (1998), Thermochronological evidence for the movement of the Ailao Shan-Red River shear zone: A perspective from Vietnam, *Geology*, *26*, 887–890.

Wang, Y. J., H. Cheng, R. L. Edwards, Z. S. An, J. Y. Wu, C.-C. Shen, and J. A. Dorale (2001), A high-resolution absolute-dated late Pleistocene monsoon record from Hulu Cave, China, *Science*, *294*, 2345–2348.

Webster, P. J., V. O. Magana, T. N. Palmer, J. Shukla, R. A. Tomas, M. Yanai, and T. Yasunari (1998), Monsoons: Processes, predictability, and the prospects for prediction, *J. Geophys. Res.*, *103*, 14,451–14,510.

Wernicke, B. P. (1990), The fluid crustal layer and its implications for continental dynamics, in *Exposed Cross-Sections of the Continental Crust*, *NATO ASI Ser., Ser. C*, vol. 317, edited by M. H. Salisbury and D. M. Fountain, pp. 509–544, Springer, New York.

Wheeler, P. J. (2000), Cenozoic basin formation in SE Asia, Ph.D. thesis, 246 pp., Univ. of Cambridge, Cambridge, U.K.

Wobus, C. W., K. V. Hodges, and K. X. Whipple (2003), Has focused denudation sustained active thrusting at the Himalayan topographic front?, *Geology*, *31*, 861–864.

Xie, X., S. T. Li, W. L. Dong, and Q. M. Zhang (1999), Overpressure development and hydrofracturing in the Yinggehai basin, South China Sea, *J. Pet. Geol.*, *22*, 437–454.

Xie, X., S. Li, W. Dong, and Z. Hu (2001), Evidence for episodic expulsion of hot fluids along faults near diapiric structure of the Yinggehai basin, South China, *Mar. Pet. Geol.*, *18*, 715–728.

Xie, X., S. Li, H. He, and X. Liu (2003), Seismic evidence for fluid migration pathways from an overpressured system in the South China Sea, *Geofluids*, *3*, 245–253.

Yan, P., D. Zhou, and Z. Liu (2001), A crustal structure profile across the northern continental margin of the South China Sea, *Tectonophysics*, *338*, 1–21.

Zhang, P., P. Molnar, and W. R. Downs (2001), Increased sedimentation rates and grain sizes 2–4 Myr ago due to the influence of climate change on erosion rates, *Nature*, *410*, 891–897.

Zhong, Z., L. Wang, B. Xia, W. Dong, Z. Sun, and Y. Shi (2004), The dynamics of Yinggehai basin formation and its tectonic significance, *Acta Geol. Sin.*, *78*, 1–7.

Zhou, D., H. Chen, S. Wu, and H. Yu (2002), Opening of the South China Sea by dextral splitting of the east Asia continental margin, *Acta Geol. Sin.*, *76*, 180–190.

Zuber, M. T., E. M. Parmentier, and R. C. Fletcher (1986), Extension of continental lithosphere: A model for two scales of basin and range deformation, *J. Geophys. Res.*, *91*, 4826–4838.

P. D. Clift, School of Geosciences, Meston Building, Kings College, University of Aberdeen, Aberdeen, AB24 3UE, UK. (p.clift@abdn.ac.uk)

Z. Sun, Key Laboratory of Marginal Sea Geology, South China Sea Institute of Oceanology, Chinese Academy of Sciences, 164 Xingangxi Road, Guangzhou 510301, China.